

DOE/ID/12779--T1

Development of Novel Active Transport Membrane Devices

Phase I Final Report

by

Daniel V. Laciak
Robert Quinn
George S. Choe
Philip J. Cook
Fu-Jya Tsai

RECEIVED

FEB 28 1996

OSTI

August 1994

Work Performed Between 31 October 1988 and 31 January 1994
Under Cooperative Agreement No. DE-FC36-89ID12779

Prepared for

United States Department of Energy
Golden Field Office, Golden Colorado
Sponsored by the Office of the Assistant Secretary
for Energy Efficiency and Renewable Energy

Office of Industrial Technology
Washington, D.C.

Submitted by

Air Products and Chemicals
7201 Hamilton Boulevard
Allentown, PA 18195-1501

MASTER

da
DISTRIBUTION OF THIS DOCUMENT IS UNLIMITED

DISCLAIMER

This report was prepared as an account of work sponsored by an agency of the United States Government. Neither the United States Government nor any agency thereof, nor any of their employees, makes any warranty, express or implied, or assumes any legal liability or responsibility for the accuracy, completeness, or usefulness of any information, apparatus, product, or process disclosed, or represents that its use would not infringe privately owned rights. Reference herein to any specific commercial product, process, or service by trade name, trademark, manufacturer, or otherwise does not necessarily constitute or imply its endorsement, recommendation, or favoring by the United States Government or any agency thereof. The views and opinions of authors expressed herein do not necessarily state or reflect those of the United States Government or any agency thereof.

Development of Novel Active Transport Membrane Devices

Phase I Final Report

by

Daniel V. Laciak

Robert Quinn

George S. Choe

Philip J. Cook

Fu-Jya Tsai

August 1994

**Work Performed Between 31 October 1988 and 31 January 1994
Under Cooperative Agreement No. DE-FC36-89ID12779**

Prepared for

**United States Department of Energy
Golden Field Office, Golden Colorado
Sponsored by the Office of the Assistant Secretary
for Energy Efficiency and Renewable Energy**

**Office of Industrial Technology
Washington, D.C.**

Submitted by

**Air Products and Chemicals
7201 Hamilton Boulevard
Allentown, PA 18195-1501**

Foreword

In 1988 Air Products and Chemicals entered into a Cooperative Agreement with the United States Department of Energy to develop "Active Transport" (AT) gas separation membranes recently discovered in our Corporate laboratories. Active Transport systems exploit chemical complexation reactions between the membrane and specific contaminant gases and thus are significantly more selective than commercial (i.e. solution-diffusion) polymer membranes. Air Products has identified Active Transport materials which selectively permeate carbon dioxide from mixtures with methane and hydrogen, hydrogen sulfide from mixtures with carbon dioxide and methane, and ammonia from mixtures with nitrogen and hydrogen.

Two significant advances in ATM technology were made during Phase IA of this Cooperative Agreement. APCI successfully translated the gas-reactive chemistry of molten salts and molten salt hydrate liquid membranes into the solid state by synthesizing new polyelectrolyte compositions. Second, APCI demonstrated that polyelectrolytes could be fabricated as thin film composite membranes in which the ATM component is stabilized on a microporous support fiber. Such composites were operated at pressures up to 1000 psi and were stable over 3 weeks of continuous testing. In Phase IA Air Products fabricated and evaluated spiral-wound thin film composite lab scale modules of NH_3 and CO_2 selective ATMs. These prototype modules displayed high permselectivity at low pressures, however, significant concentration polarization effects were observed under laboratory simulated process conditions. The major objective of this, the final segment of Phase I (Phase IB), was to demonstrate that ATMs could be fabricated in the commercially viable form of a hollow fiber device exhibiting permselectivity for separating carbon dioxide from mixtures with methane. Such membranes could be used for:

- permeating CO_2 from natural gas
- permeating CO_2 from landfill gas
- permeating CO_2 from wastewater treatment offgas

The task schedule for the Phase IB contract period is shown in Figure i. Major accomplishments for this contract period included:

- Established substrate polymer selection criteria and identified a candidate material.
- Established the effect of fiber spinning variables on substrate fiber properties and produced a hydrocarbon-resistant fiber with tunable surface porosity in the range 100 - 1000Å.
- Demonstrated concept feasibility by fabricating lab-scale, ATM composite hollow fiber membrane modules incorporating non-optimized substrates that were stable to 1000 psi and for at least 50 days of continuous operation.
- Estimated that an optimized ATM system (i.e., one which meets all performance and cost targets) could upgrade subquality natural gas (6% CO₂) for approximately 20% less than the cost of conventional (DEA) acid gas scrubbing technology.
- Identified technical hurdles that require resolution prior to further developing and commercializing Active Transport membranes.

These accomplishments are discussed in detail in Chapters III-VII. A general summary and recommendations for additional work are contained in Chapter VIII.

TASK	1992			1993												1994			
	Aug	Sep	Oct	Nov	Dec	Jan	Feb	Mar	Apr	May	Jun	Jul	Aug	Sep	Oct	Nov	Dec	Jan	
SUBSTRATE DEVELOPMENT																			
Spinning Eq. Setup																			
Spinning Studies																			
Fiber Characterization																			
COATING																			
Equipment Setup																			
Dip-coating / Module Fab.																			
TESTING																			
Equipment Setup																			
Lab Tests																			
COMMERCIAL DEVELOP. & PROCESS ENGINEERING																			
REPORTING																			
Quarterly Reports																			
Phase IB Report																			
MILESTONE: HF LAB MODULE																			

Figure i: Program Schedule

Figure 1A

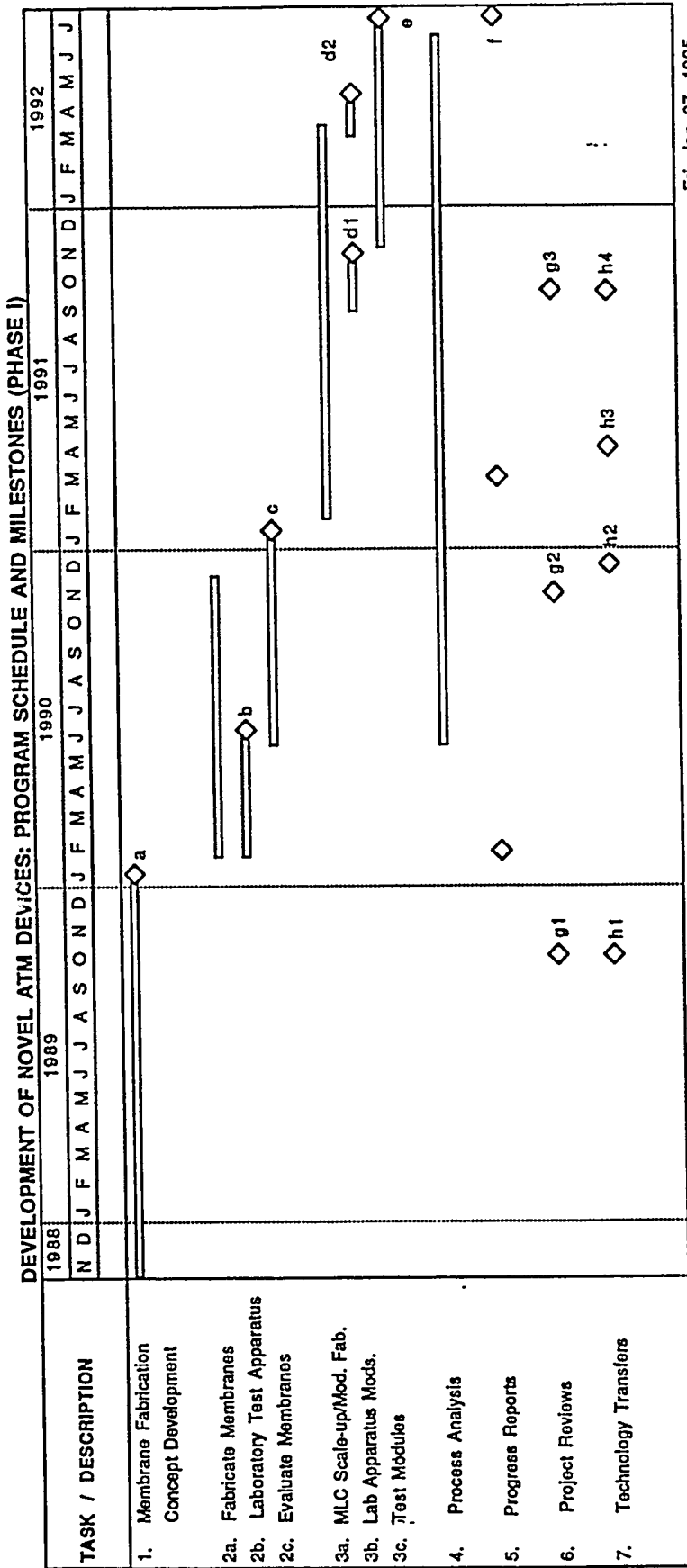


TABLE OF CONTENTS

I. Executive Summary.....	1
II. Program Overview	3
1.0 Introduction.....	3
2.0 Background.....	4
3.0 Historical Perspective - Air Products Work in AT Membranes	13
4.0 Phase IA Accomplishments	15
5.0 Technical Focus	18
III. Substrate Fiber Development.....	20
1.0 Introduction.....	20
2.0 Experimental.....	22
3.0 Result and Discussions	24
4.0 Summary and Recommendations	35
IV. Composite Membrane Development	37
1.0 Physical Properties of Coating Solutions.....	37
2.0 Coatability of Planar Substrate Coupons	41
3.0 Hollow Fiber Module Fabrication and Evaluation	43
4.0 Summary and Recommendations	72
V. Recent Advances in the Development of Active Transport Materials.....	76
1.0 Influence of H ₂ O Vapor on ATM Permeation Properties	76
2.0 Assessment of H ₂ S Reactivity of ATM Membranes.....	91
3.0 Discovery of New "High Performance" ATMs	103
VI. Process Application Development and Technology Benefits -	109
Upgrading Subquality Natural Gas.....	109
1.0 Computer Modeling of Active Transport Membranes	109
2.0 ATM Process for Upgrading Natural Gas	113
3.0 Recommendations.....	117
VII. Commercial Opportunities	122
1.0 Upgrading Subquality Natural Gas.....	122
2.0 CO ₂ - Selective ATM: Other Opportunities.....	135
3.0 Ammonia-Selective ATM Materials	138
VIII. Technology Development Status and Overall Recommendations	145

List of Figures

Figure 2-1	Passive vs. Active Mechanisms	6
Figure 2-2	Cross Section of an Immobilized Liquid, Facilitated-Transport Membrane Containing a Mobile Carrier Species	7
Figure 2-3	Schematic of Possible Transport Pathways for a Solid-State Membrane Containing Immobilized Active Sites	10
Figure 2-4	Pressure Dependence of Permeance and Selectivity of an Active Transport Membrane	12
Figure 2-5	Cross Section of a Multilayer Composite Membrane.....	16
Figure 3-1	Fiber Spin Line Schematic.....	23
Figure 3-2	Effect of Coagulation Bath Temperature on Permeance	33
Figure 4-1	Viscosity of ATM Coating Solutions	39
Figure 4-3	Schematic Representation of a Dip Coating Process.....	44
Figure 4-4	Schematic Representation of a Continuous Meniscus Coating Process..	45
Figure 4-5	Lab-Module Potting Arrangement.....	47
Figure 4-6	Apparent Manufacturing Defects of SUB1 and SUB2 Supports.....	48
Figure 4-7	Representative Cross Section of ATM-Coated SUB1	48
Figure 4-8	Effect of Feed Pressure on Performance.....	56
Figure 4-9	Performance on SUB2 Substrate	58
Figure 4-10	Performance Comparison: Bore-Side Sweep vs. No Sweep	59
Figure 4-11	Effect of P/Po on Performance	61
Figure 4-12	Stability of Lab-Scale Hollow Fiber ATM Modules	63
Figure 4-13	Lifetime/H ₂ S Stability of Hollow Fiber ATM	64

Figure 4-14	Schematic Representation of Defect Model	66
Figure 4-15	Comparison of Polysulfone-Supported PVBTAF Planar Coupons and Hollow Fiber Lab Modules.....	73
Figure 5-1	Chemical Complexation of CO ₂ by TMAF • nH ₂ O	77
Figure 5-2	Thermal Decomposition of PVBTAF and EXTM6-4	80
Figure 5-3	Proton NMR Spectra of PVBTAF and EXTM6-4.....	81
Figure 5-4	H ₂ O Absorption by PVBTAF and EXTM6-4 at 25°C Repeat Unit Basis	84
Figure 5-5	H ₂ O Absorption by PVBTAF and EXTM6-4 at 25°C Fluoride Basis	85
Figure 5-6	Permselectivity of a PVBTAF/Polysulfone Membrane as a Function P/Po	87
Figure 5-7	Selectivity and H ₂ O Absorption of PVBTAF	88
Figure 5-8	Selectivity and H ₂ O Absorption of EXTM6-4.....	89
Figure 5-9	Ionic Strength of PVBTAF and EXTM6-4.....	90
Figure 5-10	H ₂ S Permeance of a PVBTAF Composite as a Function of H ₂ S Pressure	93
Figure 5-11	CO ₂ Permeance of a PVBTAF Composite as a Function of CO ₂ Pressure.....	94
Figure 5-12	Lifetime of a PVBTAF Composite Membrane.....	97
Figure 5-13	¹ H NMR Spectra of PVBTAF Before and After Exposure to CO ₂	98
Figure 5-14	¹³ C MASNMR of PVBTAF Before and After Exposure to H ₂ S.....	101
Figure 5-15	Effect of ATM-AT Salt Blends on CO ₂ Permeance	105
Figure 5-16	CO ₂ Permeance of EXTM6-4 Composite Membranes as a Function of AT Salt Concentration.....	106
Figure 5-17	H ₂ S Permeance of EXTM6-4 Composite Membranes as a Function of AT Salt Concentration.....	108

Figure 6-1	Experimental and Model Predicted CO ₂ Permeance of PVBTAF MLC at 34°C	111
Figure 6-2	Experimental and Model Predicted CO ₂ and CH ₄ Permeance as a Function of P/Po	112
Figure 6-3	Process Flow Diagram: CO ₂ Separation from Natural Gas by ATMs...	114
Figure 6-4	Number of Modules	115
Figure 6-5	Compressor Power	116
Figure 6-6	Hydrocarbon Loss	118
Figure 6-7	Economics of ATM and DEA Systems for CO ₂ Separation from Natural Gas	119
Figure 6-8	Comparison of Laboratory Properties to Targets.....	120
Figure 7-1	U.S. Utilization of Natural Gas Production Capability	124
Figure 7-2	Natural Gas Prices in the U.S. - 1991	129
Figure 7-3	Generic Ethylene Oxide Process.....	140

List of Tables

Table 3-1	Comparison in Spinning Processability	25
Table 3-2	Physical Properties of Candidate Polymers	25
Table 3-3	Hydrocarbon Resistance of PAI.....	26
Table 3-4	Chemical Resistances of Candidate Fibers.....	28
Table 3-5	Effect of Solvent Exposure on PAI Fiber Permeance.....	29
Table 3-6	Tensile Strength Tests of Fibers	30
Table 3-7	Effect of Air Gap on Fiber Permeance	31
Table 3-8	Environmental Effect in Air Gap on Fiber Property (Coagulation Bath Temperature 51°C).....	34
Table 3-9	Environmental Effect in Air Gap on Fiber Property (Coagulation Bath Temperature 60°C).....	35
Table 3-10	Current Status of Development	36
Table 4-1	GPC MALLS Molecular Weight Determination of Poly(vinylbenzyltrimethylammonium) and Poly(diallyldimethylammonium) AT Polymers.....	38
Table 4-2	Contact Angle of ATM Solvents with Substrate Polymers	40
Table 4-3	Dynamic Contact Angle Between ATM Coating Solutions and PAI Fiber.....	41
Table 4-4	Permselectivity of a PVBTAF/Polysulfone Flat Sheet Composite Membrane as a Function of CO ₂ Pressure (12484-76B).....	42
Table 4-5	Permselectivity of a PVBTAF/PAI Planar Coupon as a Function of CO ₂ Pressure (12484-82).....	42
Table 4-6	Summary: Permselectivity of PVBTAF-Coated SUB1 and SUB2 Modules.....	51
Table 4-7	Temperature Dependence of Permselectivity	60

Table 4-8	Comparison of Typical Planar and Hollow Fiber Membranes	65
Table 4-9	Permselectivity Basis for Defect Model	66
Table 4-10	Comparison of Experimental and Model Predicted Permselectivity for an ATM Hollow Fiber Module ($x = 0.9983$)	67
Table 4-11	Performance of EXTM6-4 Coated PAI Hollow Fiber Modules	68
Table 4-12	Summary: Permselectivity of EXTM8-Coated PAI Modules	69
Table 5-1	NMR Peak Assignments.....	79
Table 5-2	Water Content of "Dry" PVBTAF and EXTM6-4.....	82
Table 5-3	H ₂ O Absorption by PVBTAF and EXTM6-4 at 25°C.....	83
Table 5-4	H ₂ S Permselective Properties of PVBTAF Membranes at 22°C.....	92
Table 5-5	H ₂ S Permselectivity vs. Time for a PVBTAF Composite at 30°C	96
Table 5-6	H ₂ S Permselectivity vs. Time for a PVBTAF Composite Membrane at 30°C	96
Table 5-7	CO ₂ Permselective Properties of EXTM6-4 Composites at 23°C	104
Table 5-8	H ₂ S Permselective Properties of EXTM6-4 Membranes at 30°C.....	107
Table 7-1	U.S. Natural Gas Consumption and Production (Dry Gas Basis).....	123
Table 7-2	U.S. Natural Gas Production and Reserve Data	126
Table 7-3	Non-Hydrocarbon Impurity Estimates for U.S. Natural Gas Reserves....	127
Table 7.4	Natural Gas Treatment Costs at 10 MMSCFD	128
Table 7-5	Acid Gas Removal Market Players.....	131
Table 7-6	Acid Gas Removal - Dominant Technologies, U.S. 1984-1995.....	132
Table 7-7	Technology Comparison of Amine and Membrane Technologies	133
Table 7-8	Ethylene Oxide Plant - CO ₂ Removal Service.....	139

List of Abbreviations and Acronyms

AGR	Acid gas removal
ATM	Active Transport Membrane
l	Membrane thickness
P	Permeability
P/l	Permeance
P/P _o	Actual H ₂ O vapor pressure/saturated H ₂ O vapor pressure
PAI	Polyamideimide
PAN	Polyacrylonitrile
PSA	Pressure swing adsorption
PVBTAf	Poly(vinylbenzyltrimethylammonium fluoride)
PDMS	Poly (dimethylsiloxane)
TMAF	Tetramethylammonium fluoride
α	Selectivity
UDEL	Polysulfur
Ultem	Polyetherimide

I. Executive Summary

The main objective of this program was to identify and develop through proof of concept, a technique for fabricating Active Transport Materials* (ATM) into lab-scale membrane devices. Air Products met this objective by applying thin film, multilayer fabrication techniques to support the AT material on a substrate membrane. In Phase IA, spiral-wound and later in Phase IB, hollow fiber membrane modules were fabricated and evaluated. These nonoptimized devices were used to demonstrate the AT-based separation of carbon dioxide from methane, hydrogen sulfide from methane, and ammonia from hydrogen. During this period, Air Products determined that a need exists for a more cost efficient and less energy intensive process for upgrading subquality natural gas. Air Products estimated the effectiveness of ATM for this application and concluded that an optimized ATM system could compete effectively with both conventional acid gas scrubbing technology and current membrane technology. In addition, the optimized ATM system would have lower methane loss and consume less energy than current alternative processes. Detailed results were communicated to DOE through a series of interim reports.

During the last budget period, Air Products made significant progress toward the ultimate goal of commercializing an advanced membrane for upgrading subquality natural gas. The laboratory program focused on developing a high performance hollow fiber substrate and fabricating and evaluating ATM-coated lab-scale hollow fiber membrane modules. Selection criteria for hollow fiber composite membrane supports were developed and used to evaluate candidate polymer compositions. A poly(amide-imide), PAI, was identified for further study. A research spinning line was constructed and used to establish the effect of spinning process variables on fiber performance. Conditions were identified which produced microporous PAI support membrane with tunable surface porosity in the range 100-1000Å. The support fibers exhibited good hydrocarbon resistance and acceptable tensile strength though a higher elongation may ultimately be desirable. ATM materials were coated onto commercial and PAI substrate fiber. Modules containing 1-50 fibers were evaluated for permselectivity, pressure stability, and lifetime. Several nonoptimized modules exhibited permselectivity comparable to planar thin film composite membranes supported on polysulfone. In general, higher flux modules would be needed to achieve commercially attractive economics.

Concurrent with but separate from this Cooperative Agreement, Air Products has maintained an active program to further develop the chemistry of its ATM materials. Results from this program

*Active Transport materials are Air Products' proprietary advanced facilitated transport gas separation polymers.

were incorporated into a semi-empirical computer model of the ATM permeation mechanism which was used to determine process economics for the natural gas application. Several technical issues related to the ultimate commercialization of ATM technology were identified. These issues include an apparent reactivity with hydrogen sulfide and, most importantly, a strong dependence of the carbon dioxide permselectivity on the concentration of water vapor in the feed gas stream. New ATM compositions which exhibited a 10-fold improvement in carbon dioxide flux while maintaining high carbon dioxide/methane selectivity were identified. Planar composite coupons of these compositions meet preliminary carbon dioxide flux and selectivity targets, however, initial indications are that they will be subject to the same commercialization challenges identified previously.

Phase IA also assessed the potential for ammonia separation membranes and modules. While excellent permselectivity was achieved for laboratory devices and it is believed that laboratory properties could eventually be scaled to a commercial system, the market potential for such membranes does not appear large enough to warrant the substantial development investment to commercialize these membranes.

Based on the results of this program, Air Products recommends a follow-on program with the task elements listed below.

- Continued efforts to assess the commerciality of ATM as related to the issues of (a) the water dependence of the carbon dioxide flux and selectivity and (b) hydrogen sulfide reactivity of the ATM component.
- Continued computer modeling of the ATM permeation mechanism, especially in regard to adequately incorporating into the model the water vapor dependence of the permselectivity.
- Continued process engineering and economic analysis to (a) further quantitate the benefits of an ATM-based natural gas purification process and (b) set performance targets for the ATM.
- Address issues related to scale-up and optimization of substrate fiber.
- Field testing of substrate and composite membranes.
- Continued commercial development activities to coordinate field testing and maintain industry contacts.

II. Program Overview

1.0 Introduction

In a recent research needs assessment performed for the U.S. Department of Energy,¹ the membrane based separation of acid gases from hydrocarbons and H₂ was ranked "high" in importance (8 out of a possible 10) and with "good" prospects for success. The study further pointed out that high selectivity materials, $\alpha(\text{H}_2\text{S}/\text{CH}_4) > 45$ and $\alpha(\text{CO}_2/\text{H}_2) > 20$, are needed to compete effectively with alternative technologies. Since 1983, Air Products has pioneered the development of active transport (AT) membranes (referred to in the literature as "facilitated" transport membranes) for the removal of acid gases from process streams. AT membranes, unlike polymeric membranes, selectively permeate acid gases by exploiting two properties:

- (1) the membranes exhibit a specific and reversible chemical reactivity with acid gases, and
- (2) the solubility of non-acid gases in the membranes is very low.

The reversible reactivity of the membranes result in enhanced permeation of acid gas while the membranes exhibit barrier properties to non-acid gases due to their low solubilities.

The AT materials under development through this Cooperative Agreement are polyelectrolytes. Polyelectrolytes are ionic polymers which have a high ionic content, up to one ionic unit per polymer repeat unit. Air Products has demonstrated that certain polyelectrolytes exhibit reversible reactivity with respect to gases and possess absorption capacities in excess of 1 mol gas / mol polyelectrolyte. In addition, we have shown that acid gas permeabilities increase with decreasing feed pressure, an observation which is consistent with active transport of the gas. In contrast, H₂ and CH₄ permeabilities are independent of feed pressure and are low. These gases cannot react with the polyelectrolyte membrane and, due to the ionic character of polyelectrolytes, H₂ and CH₄ are almost insoluble in the membrane. The performance of small planar sheet membranes was favorable. Acid gas

¹ "Membrane Separation Systems - A Research & Development Needs Assessment" by the Department of Energy Membrane Separation Systems Research Needs Assessment Group; Volume II, March 1990.

permeances (CO₂ and H₂S) were relatively high: 1.0 - 0.7x10⁻⁶ cm³/cm²•s•cmHg for CO₂ and 3.0 - 30x10⁻⁶ cm³/cm²•s•cmHg for H₂S. The selectivity of acid gas to H₂ and CH₄ selectivities were exceptional: α(CO₂/H₂) = 10 - 60; α(CO₂/CH₄) = 50 - 700; α(H₂S/CH₄) = 260 to >2000. These properties are not observed for conventional polymeric materials and may have considerable practical value in processing streams containing CO₂ and/or H₂S such as subquality natural gas.

2.0 Background

Gas transport in conventional polymeric membranes occurs by a "passive" solution-diffusion mechanism; that is, gases dissolve in the polymer membrane at the high pressure (feed) side and diffuse in a concentration gradient to the low pressure side where they are liberated to the permeate stream. The intrinsic measure of a material's resistance to gas transport is termed the standard permeability, P. It is the flow rate of gas (Q) permeating a membrane of unit cross-sectional area (A), unit thickness (ℓ), and unit partial pressure driving force (ΔP):

$$P = \frac{Q \cdot \ell}{A \cdot \Delta P} = \frac{\text{cc(STP)} \cdot \text{cm}}{\text{cm}^2 \cdot \text{s} \cdot \text{cmHg}}$$

It has become customary to represent permeability in Barrer units where
1 Barrer = 10⁻¹⁰ cc•cm/cm²•s•cmHg.

When the membrane thickness is unknown or ill-defined (such as in an asymmetric membrane), it is useful to refer to the permeance, P₀/ℓ of the membrane

$$\text{permeance} = P/\ell = \text{cc}/\text{cm}^2 \cdot \text{s} \cdot \text{cmHg}$$

From a practical point of view, permeance is the property which predominantly controls the amount of membrane area required to effect the separation of a given amount of gas and is related to the system capital investment.

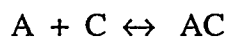
Selectivity of a polymer for two species, A and B, is defined as the ratio of the standard permeabilities of the two species through the polymer.

$$\text{selectivity (A/B)} = \alpha(\text{A/B}) = P(\text{A})/P(\text{B}) = [P/\ell](\text{A}) / [P/\ell](\text{B})$$

The membrane selectivity controls the amount of product lost to the permeate. Higher selectivities result in lower product losses and usually improved economics. Low selectivity can sometimes be compensated for by staged processes (multiple membranes connected through interstage compression) but these are more complicated and usually more energy and capital intensive than single stage processes.

Active or facilitated transport gas separation membranes capitalize on chemical reactions or interactions between a species in the membrane and the gaseous component of interest. This provides an additional transport pathway for that gas as shown in Figure 2-1. Both gases A and B permeate the facilitated transport membrane via a solution-diffusion mechanism. However, gas A can react with a species in the membrane and thus has a second mechanism for permeation. As a result, active transport membranes can have permeability and selectivity considerably greater than polymeric membranes.

Several types of active transport membranes have been previously investigated. The most widely studied have been immobilized-liquid, mobile carrier facilitated membranes (ILMs). These membranes consist of a solution of a chemically reactive "carrier" and a solvent immobilized in a microporous polymer matrix. This mode of facilitated transport is shown in Figure 2-2. At the feed side of the membrane, gas A reacts reversibly with carrier molecule C (which is dissolved in a solvent) to form a carrier-gas complex AC:

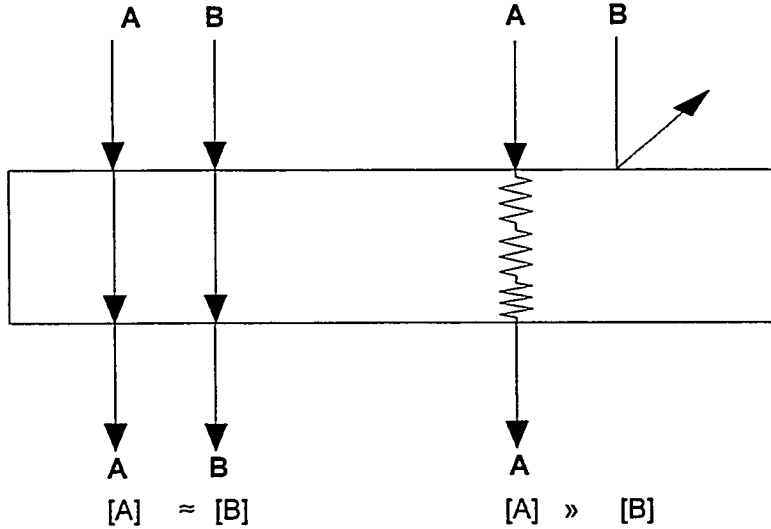


This complex diffuses in a concentration gradient to the permeate side of the membrane where it dissociates. Uncomplexed carrier C diffuses back to the feed side of the membrane to complete the cycle while gas A is liberated to the permeate stream. Nonreactive component B still permeates the membrane by a conventional solution-diffusion mechanism (as does A); however, under conditions favorable to the facilitation reaction, (which depend on the thermodynamics and kinetics of the A+C reaction), a very high flux of A relative to B can be obtained and hence, a very high selectivity, $\alpha(A/B)$. Examples of this type of active transport are the selective removal of CO₂ from streams containing O₂, N₂, and CH₄,^{2,3} the

² W.J. Ward and W.L. Robb, *Science*, 1981 (1967).

³ J.D. Way, R.D. Noble, D.L. Reed, and G.M. Ginley, *AIChE Journal*, 33(3), 480 (1987).

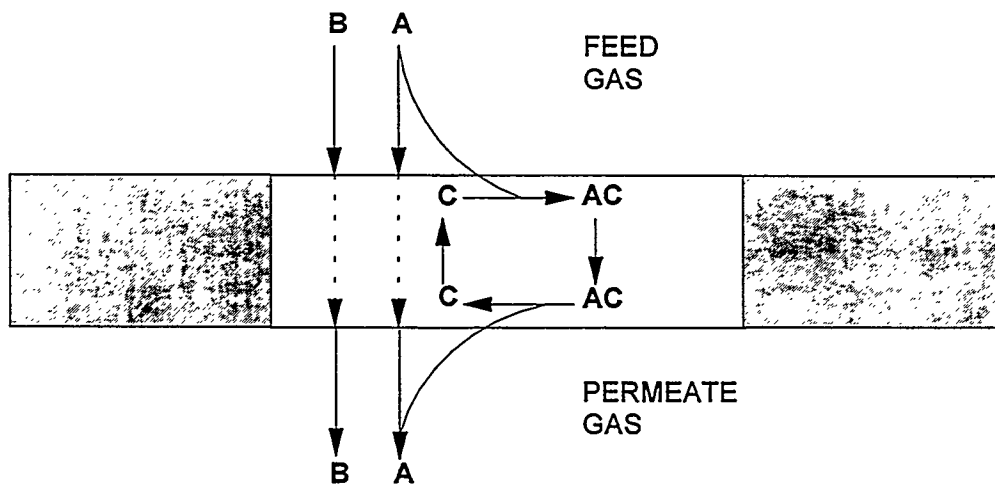
Figure 2-1
Passive vs. Active Mechanisms



Passive Pathway
(Solution-Diffusion)

Reactive Pathway
(Active-Transport)

Figure 2-2
***Cross Section Of An Immobilized Liquid,
Facilitated-Transport Membrane
Containing A Mobile Carrier Species***



selective removal of H₂S, CO and NO from various streams,^{4,5} and the separation of oxygen from air.⁶ While ILMs have been investigated since the 1960's and are reported in the literature to have shown impressive selectivities, there are a number of technical hurdles which have prevented such membranes from gaining commercial acceptance. Some of these are:

- **Fabrication of immobilized liquid membranes which are dimensionally stable to the high process pressures.** Many commercial processes operate at pressures greater than 300 psi and often in the range of 1000 to 2000 psi. Immobilized liquid membranes (ILMs) depend on capillary forces to maintain integrity. All other factors being equal, the pore size of the support membrane determines the maximum operating pressure of the ILM. The unavailability of inexpensive, defect-free, high porosity matrices with a narrow distribution of very small pores has hindered the commercialization of ILMs.
- **Identification of stable carrier species.** Facilitated transport membranes contain chemically reactive species which can either degrade over time or undergo side reactions with other components; the latter is especially true if the membrane is contacted with commercial process streams.
- **Identification of suitable nonvolatile solvents.** Membrane life can be limited by the rate of solvent evaporation. Solvent recovery and replenishment systems have been designed into immobilized liquid facilitated transport membrane modules,^{7,8,9} but apparently have not been practical. Solvent loss from the membrane is not only a membrane performance and cost issue, but also leads to contamination of product and vent streams.
- **Saturation of the chemical pathway.** Facilitated transport membranes rely on chemical reactions for their permselectivity. For many active transport systems the

⁴ J.D. Way, R.D. Noble, T.M. Flynn, and E. Dendy Sloan, *J. Membrane Sci.*, **12**, 239 (1982).

⁵ C.A. Koval, R.D. Noble, J.D. Way, B. Louie, Z.E. Reyers, B.R. Bateman, G.M. Honn and D.L. Reed, *Inorg. Chem.*, **24**, 147 (1985).

⁶ J.A.T. Norman, G.P. Pez and D.A. Roberts, in "Oxygen Complexes and Oxygen Activation by Transition Metals", A. E. Martell and D. T. Sawyer, eds., Plenum Publ. Corp. 1988 and references therein.

⁷ S.L. Matson, U.S. Pat. No. 4,119,408 (1978).

⁸ G.E. Walnut and S.L. Matson, U.S. Pat. No. 4,187,086 (1980).

⁹ S.L. Matson, U.S. Pat. No. 4,174,374 (1979).

chemical pathway is saturated at relatively low pressure and consequently the permselectivity at commercial conditions may often be no better than conventional (passive transport) polymer membranes.

These areas are the focus of current research in several laboratories. Some efforts involve synthesis of more robust carriers for acid gases¹⁰ and oxygen¹¹. Other research centers on the development of new devices, such as Hollow Fiber Contained Liquid Membranes, designed to minimize the negative features of traditional facilitated membranes.¹² Interest has also focused on facilitated transport of gases through solid membranes which contain immobilized reactive sites. Figure 2-3 shows two transport mechanisms which have received attention. In pathway 1, gas molecules bind directly to specific fixed sites, O, within the membrane matrix. A bound gas molecule can then exchange or "hop" to a nearby empty site. As this process is repeated, the gas is effectively transported across the membrane with a concurrent "flux" of empty sites in the opposite direction. The second pathway (2) consists of solubilization of a gas within a nonspecific matrix site, (\square), diffusion to and binding at a reaction specific site, (O), and dissolution back into the matrix. Note that transport in conventional polymeric membranes is simply transport between non-specific sites. Barrer¹³ has published a mathematical analysis of transport in such "fixed-site" membranes. Nishide¹⁴ *et al.* have published evidence that active transport of O₂ may occur in polymeric membranes that contain fixed oxygen complexes, most likely by the second mechanism. It is only recently that evidence for a direct site-to-site transport mechanism has appeared.¹⁵

In addition to suffering some of the limitations of the immobilized liquid membranes, solid state active transport membranes face the following additional hurdle:

- **Fixed site membranes with a high concentration of sites.** Current fixed site facilitated transport membranes have a relatively low concentration of reactive sites. Performance could be improved if the site density were significantly increased.

¹⁰ C. Koval, M. Rakowski-Dubois, and R.D. Noble, "Sulfur Resistant Complexing Agents for Olefin Separations", presented at the 5th Annual Meeting of the North American Membrane Society, Lexington, KY, May 1992.

¹¹ D. Ramprasad et al., in "5th Symposium on Activation of Dioxygen and Homogeneous Catalytic Oxidation", in press.

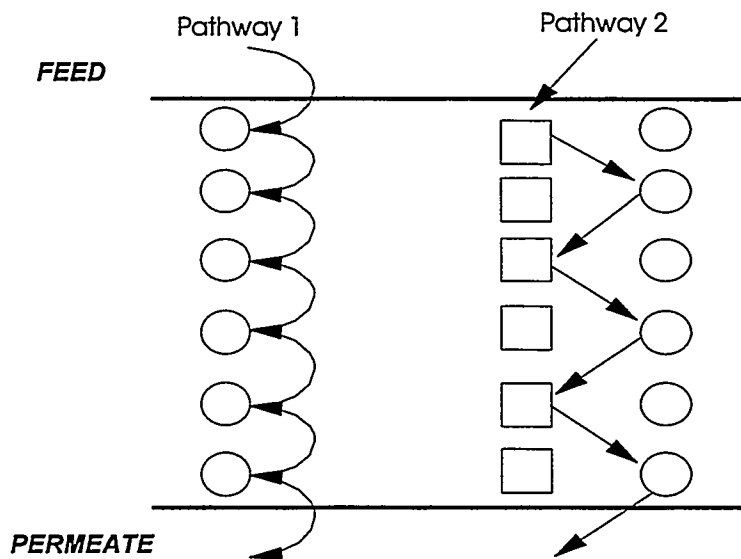
¹² S. Majumdar, A. Guha, and K.K. Sircar, *AIChE Journal*, **34**, 1135 (1988).

¹³ R.M. Barrer, *J. Membrane Sci.*, **18**, 25 (1984).

¹⁴ M. Nishide, O. Ohyanagi, O. Okadra, and E. Tsuchida, *Macromolecules*, **20**, 417 (1987).

¹⁵ S. Skinkai, K. Tarigoe, O. Manabe, and T. Kajiyama, *J. Am. Chem. Soc.*, **109**, 4458 (1987).

Figure 2-3
Schematic Of Possible Transport
Pathways For A Solid-State Membrane Containing
Immobilized Active Sites



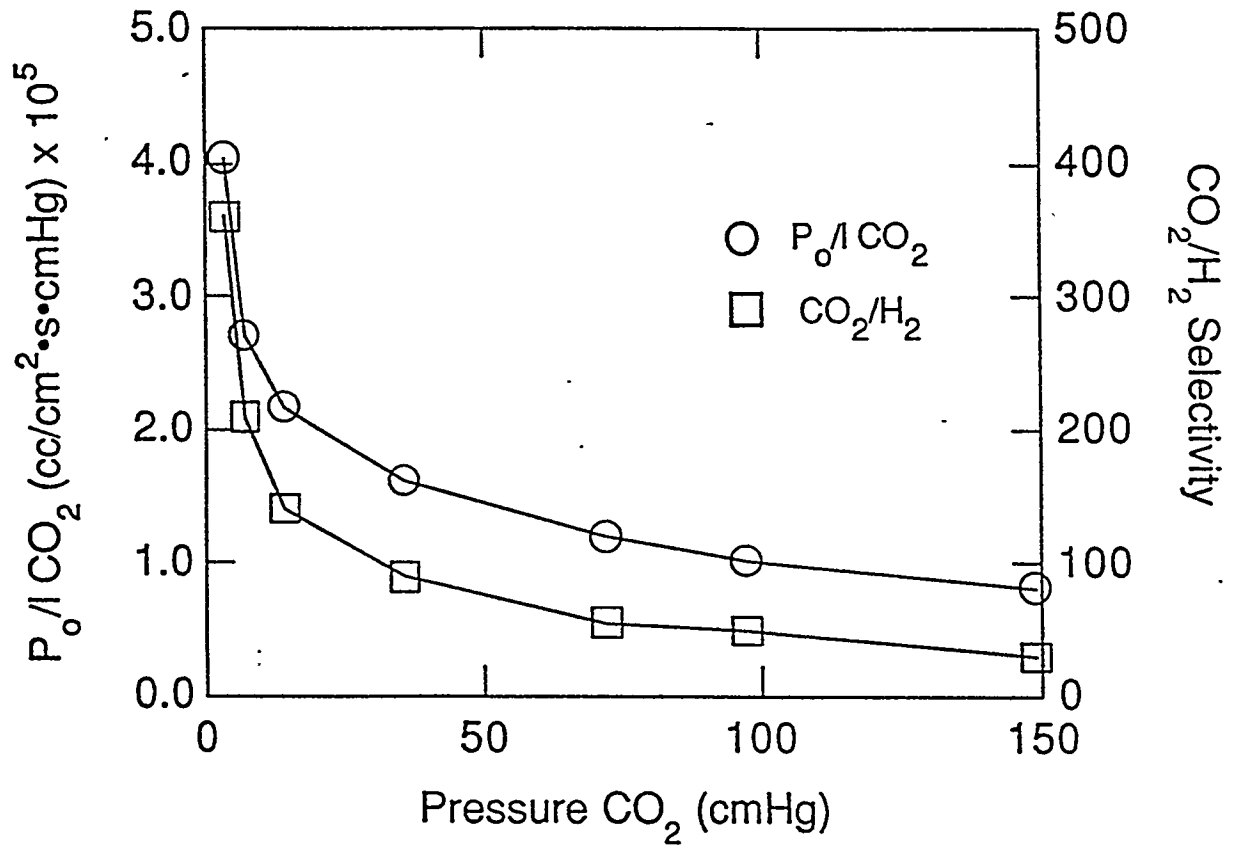
An important point to note about active transport systems in general, both of the immobilized liquid and solid types, is that, because they rely on chemical reactions between the permeant gas and a carrier species in the membrane, the permeability and permance of such membranes will be a function of the kinetics and equilibrium constant expression for the carrier-gas reaction. Because the equilibrium expression for the carrier-gas complex includes a term for the gas partial pressure, active transport membranes often exhibit a pressure dependent permeability (and permance). This behavior is shown in Figure 2-4. The permeability is greatest at low pressures where the reactive pathway is used to full advantage. As the pressure is increased, the reactive pathway becomes saturated and the permeability, which is normalized for the partial pressure driving force, decreases proportionately. Because the permeability of non-interacting gases does not depend on the pressure, the selectivity of active transport membranes also exhibits this pressure dependence, and may be no better than conventional membranes under high pressure operating conditions.

Membrane processes normally favor the highest possible operating pressures in order to maximize the amount of gas that can be processed with the minimum amount of membrane area. In contrast, the properties of AT membranes discussed above, i.e., an inverse relationship of permance and selectivity with pressure, may tend to favor lower operating pressures for AT membrane-based processes. These somewhat conflicting properties of active transport systems gives rise to the notion of an optimum operating pressure window for AT membrane-based systems.^{16,17} They also suggest that a detailed understanding of membrane operating characteristics as a function of process conditions will be required in order to design engineered systems which make optimum use of the AT membranes.

¹⁶ L.L. Kemena, R.D. Noble, and N.J. Kemp, *J. Membrane Sci.*, **15**, 259 (1983).

¹⁷ E.L. Cussler, A. Aris and A. Bhowan, *J. Membrane Sci.*, **43**, 149 (1989).

Figure 2-4
Pressure Dependence Of Permeance And Selectivity
Of An Active Transport Membrane



3.0 Historical Perspective - Air Products Work in AT Membranes

Recognizing the potential impact of membranes in general and active transport membranes in particular, Air Products in 1983 initiated a research and development program in this technology area within its Corporate Research group. This program focused on addressing many of the technical hurdles which have thus far kept gas facilitated transport systems a laboratory curiosity. Air Products initially sought to develop stable, low volatility materials which reacted reversibly with oxygen and ammonia. The program was later expanded to include the development of materials for reaction with carbon dioxide, carbon monoxide, hydrogen sulfide and water vapor.

Molten salts were the first active transport media investigated. The concept of using molten salts as active transport media brought several novel and unique features to facilitated transport. First, since molten salts are inherently liquid, no solvent was necessary. As a result, the concentration of carrier species was extremely high and there were no solvent evaporation issues. Furthermore, since molten salts are ionic, they have very low vapor pressures. The ionic nature of the molten salt media also acts to minimize the permeation of non-interacting gases by a solution-diffusion mechanism via the "salting-out effect."¹⁸ Immobilized molten salt membranes were fabricated which exhibited exceptional active transport of oxygen¹⁹ and ammonia²⁰ at 300°C. This was the first example of facilitated transport membranes which functioned at such high temperatures. Air Products was awarded patent coverage on the use of molten salt membranes for gas separation.^{21, 22}

Further work expanded the scope of molten salt facilitated membranes to include selective permeation of CO₂ and CO at near-ambient temperatures by using molten salts which contained large organic cations to lower their melting points.²² These large organic cations, however, also increased the solution-diffusion permeation of the non-interacting gases, resulting in a lower selectivity. To circumvent this problem, Air Products developed molten salt hydrate membranes. Lab tests showed immobilized liquid membranes fabricated from molten salt hydrates were extremely selective for CO₂ and H₂S over CH₄ and exhibited the

¹⁸ D.A. Palmer and R. Van Eldik, *Chem. Rev.*, **83**, 651 (1983).

¹⁹ G.P. Pez and R.T. Carlin, *J. Membrane Sci.*, **65**, 21 (1992).

²⁰ D.V. Laciak, G.P. Pez and P.M. Burban, *J. Membrane Sci.*, **65**, 31 (1992).

²¹ G.P. Pez and R.T. Carlin, U.S. Pat. No. 4,617,029 (1986).

²² G.P. Pez, R.T. Carlin, D.V. Laciak and J.C. Sorensen, U.S. Pat. No. 4,761,164 (1988).

highest reported selectivity for CO₂ over H₂.²³ The unique nature of these membranes was recognized in two U.S. Patents.^{24, 25}

By the mid 1980s Air Products had developed a variety of inherently liquid active transport materials with potential in a number of commercial applications including ammonia synthesis, merchant hydrogen production, acid gas scrubbing, and gas dehydration. Continued development of this technology required active transport materials in a form suitable for fabrication into practical membranes and separation devices. In 1985, Air Products began to synthesize "polymeric analogs" of molten salts and molten salt hydrates; namely, polyelectrolytes. Active transport polyelectrolytes consist of a polymeric backbone containing pendant cationic functionality and their associated counter ions--a polymeric salt. New compositions which showed unprecedented selectivity for ammonia over nitrogen and hydrogen were developed.²³ In 1988, Air Products was awarded two patents on these materials.^{26, 27}

In October of 1988, Air Products entered into this Cooperative Agreement with the U.S. Department of Energy, Office of Industrial Programs (DE-FC07-89ID12779). The goal of this Phase I project was to demonstrate that Air Products' proprietary Active Transport membrane materials could be fabricated into commercially practical membranes and devices. Thus far, Air Products identified, developed and evaluated composite ATM membranes, fabricated and evaluated lab-scale spiral-wound modules and refined ATM-based separation schemes for commercial processes.^{28,29}

Meanwhile, Air Products continued its independently funded active transport materials development program. In 1990, polyelectrolytes were synthesized for separating carbon dioxide and hydrogen sulfide from hydrogen and methane. The effectiveness of these materials was demonstrated as part of the Phase I program.^{28, 29} Moreover, these active transport compositions possessed high selectivity for hydrogen sulfide over carbon dioxide.

²³ D.V. Laciak, R. Quinn, G.P. Pez, J.B. Appleby and P.S. Puri, *Sep. Sci. and Tech.*, **25** 1295 (1990).

²⁴ R. Quinn, G.P. Pez and J.B. Appleby, U.S. Pat. No. 4,780,114 (1988).

²⁵ R. Quinn and G.P. Pez, U.S. Pat. No. 4,973,456 (1990).

²⁶ D. V. Laciak and G.P. Pez, U.S. Pat. No. 4,758,250 (1988).

²⁷ G.P. Pez and D.V. Laciak, U.S. Pat. No. 4,762,535 (1988).

²⁸ (a) D.V. Laciak, "Development of Novel Active Transport Membranes Devices", DE-FC07-89ID12779, interim report February 1990. (b) *ibid.* March 1991.

²⁹ J.S. Choe, L.J. Kellogg, D.V. Laciak, T.A. Shenoy, and S.C. Weiner, "Development of Novel Active Transport Membranes Devices", DE-FC07-89ID12779, interim report January 1993.

These materials are the subject of two patent applications. In 1994 Air Products received a patent on the use of polyelectrolyte membranes for the separation of acid gases.³⁰

4.0 Phase IA Accomplishments

Since November 1988 Air Products has pursued a cooperative research program with the U.S. Department of Energy-Office of Industrial Technology aimed at assessing the feasibility of commercializing ATM technology. This program included various laboratory tasks, and process and commercial development activities. Detailed results have been reported to DOE.^{28,29} Specific accomplishments from that program include:

- **Identified a composite membrane fabrication concept.** A technique whereby the active transport polyelectrolyte was supported on a microporous substrate and coated with a relatively permeable but nonselective polymer (e.g. silicone rubber) was identified and developed. Figure 2-5 shows a schematic cross-section of such a composite and an image taken by a scanning electron microscope. Fabrication of composite coupons (4 cm²) were scaled to planar sheets (1 ft²).
- **Demonstrated high pressure operation of CO₂ and NH₃-selective composite ATM coupons.** Composite AT coupons were evaluated in mixed gas streams at Air Products' laboratories as a function of gas pressure (to 1000 psi), composition, and flowrate, temperature, and, in some cases, water vapor content of the gas stream. Membrane stability was demonstrated for 30+ days of continuous operation.
- **Fabricated and evaluated lab-scale spiral wound ATM modules.** Planar composite membranes were wound into spiral elements (200 cm²) and their performance was evaluated at conditions approaching those of commercial processes. Lab tests suggested that concentration polarization effects reduced the effectiveness of the membrane module at the flow rates tested by introducing a significant gas phase resistance to permeation. This might be less of an issue in high flow rate commercial installations where the feed gas streams are better mixed.

³⁰ R. Quinn, D.V. Laciak, J.B. Appleby and G.P. Pez, "Polyelectrolyte Membranes for the Separation of Acid Gases", U.S. Pat. No. 5,336,298 (1994).

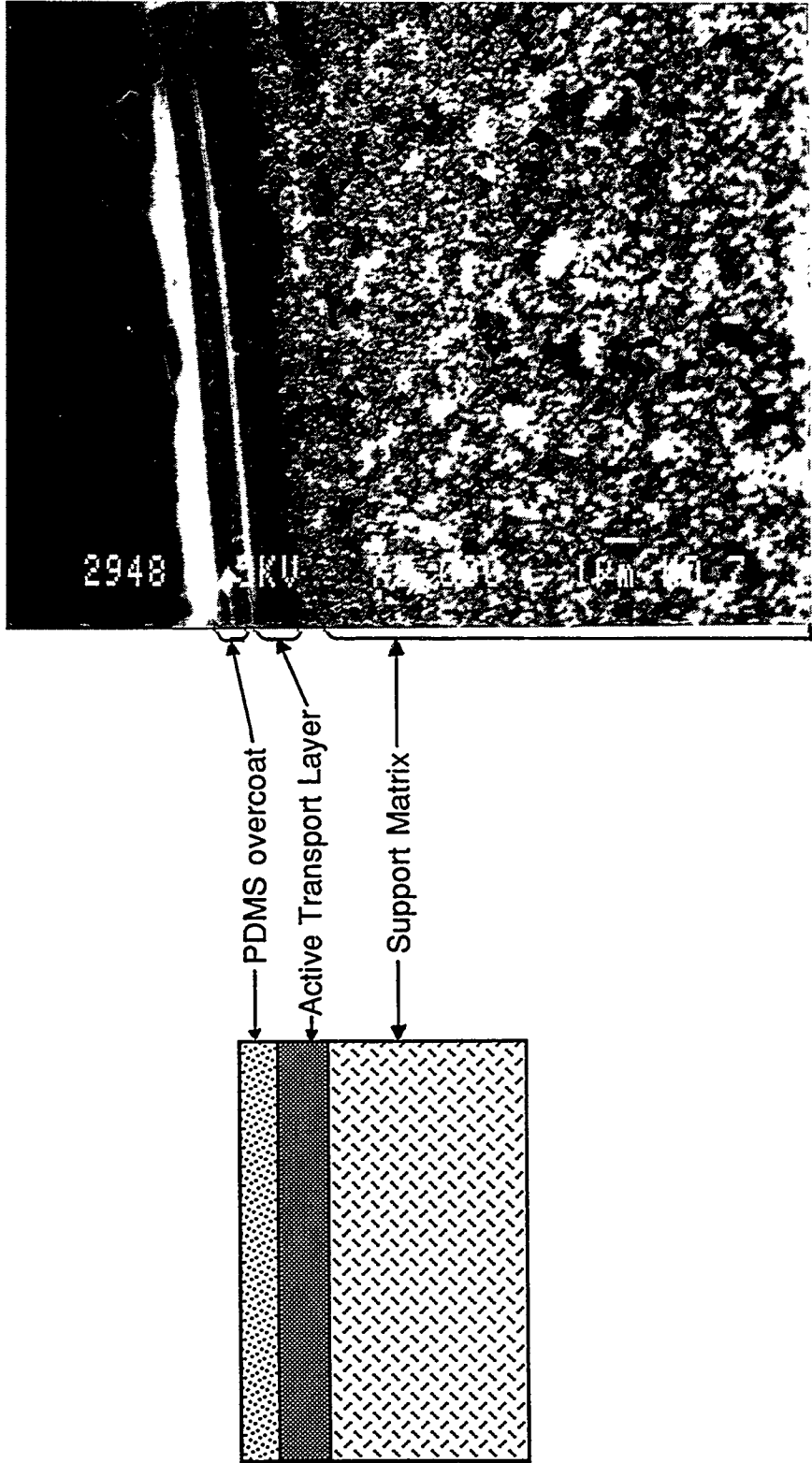


*Figure 2-5
Cross-section of a Multilayer Composite Membrane*

- **Developed detailed flow sheets for incorporating ATMs into selected commercial processes.** Process schemes were developed for utilizing ATMs and ATM-hybrids in hydrogen production via steam-methane reforming. Estimated membrane performance was used to predict mass and energy balances. Bottom-line economics showed that ATMs can be cost competitive with conventional acid gas scrubbing systems by providing an energy savings to offset the cost of capital. Several potential process schemes were identified for incorporating ATMs into ammonia synthesis plants. The ATM-based systems had both lower capital and energy costs.
- **Identified natural gas processing as a market with high potential for ATM technology.** Several markets including ammonia and urea synthesis, merchant hydrogen and syngas production, and natural gas processing were analyzed. Sizable growth is projected for natural gas production. ATM-Pressure Swing Absorption hybrids are expected to offer opportunities in the strong hydrogen market. Slow growth is forecast for domestic ammonia capacity. Energy savings was found to be an important but not a key factor in choosing among competing technologies.
- **Identified areas for further experimental work.** The permselectivity of ATMs was found to be highly sensitive to the water vapor content of the feed gas stream. The implication of this observation to projected module performance and economics will need to be assessed in any follow-on program. ATM material modifications to moderate this effect should also be sought. In addition, follow-on work should focus on increasing the CO₂ flux of the ATM composite either by thinning the ATM layer, by identifying and incorporating catalysts or both.

5.0 Technical Focus

As indicated in Section 2.2, of Chapter II, the objective of this phase of the program was to demonstrate ATM technology in a commercially feasible form. For simplicity and due to its ready accessibility, the initial demonstration of membrane and module fabrication was accomplished in flat sheet and spiral wound module form. Hollow fiber configurations, however, offer the following inherent advantages relative to flat sheet and spiral configurations:

- A hollow fiber module is inherently simpler than a spiral since it does not require the spiral's spacer components.
- Hollow fiber modules are less labor intensive and, hence, cheaper to produce.
- Hollow fiber modules provide a higher membrane packing density than spirals (often by as much as a factor of 10 or more). The higher packing density permits the design of smaller, less costly systems.

Overall, the combination of fewer components, an inherently cheaper manufacturing technology, and a lower system cost are expected to provide significantly improved economics for the membranes in hollow fiber form. While the primary focus of DOE must be on energy savings and on bringing new energy sources to the market, acceptance of this technology by the ultimate users will depend heavily on the economics of this technology. The favorable economics of hollow fibers and the strong focus of Air Products as well as DOE on technology commercialization mandated that we translate the early work conducted on flat sheets to hollow fibers.

Many years of research at Air Products (both with DOE and in our independently funded programs) have been devoted to the fabrication of composite membranes. This experience has taught us about the critical inter-relationship of the properties of the support membrane, the coating polymer properties, and the process variables of the coating process on the overall properties of a composite membrane. With the decision to fabricate the ATM in hollow fiber form, a fresh look was taken at the nature of the membrane structure, and we set out to separately optimize each of the membrane's individual components in order to maximize the

overall membrane properties for its intended end use application. Therefore, the technical program for this, the last segment of Phase I included:

- **Hollow Fiber Substrate Fiber Spinning**

The demanding process conditions of natural gas processing operations require that the composite membrane be supported on a robust support membrane. It was not apparent that commercial microporous membranes possessed acceptable properties. Therefore, this task included defining the chemical and physical characteristics for a high performance substrate, screening candidate materials, and finally formulating a spin dope and spinning fiber samples for physical and coating evaluations.

- **Composite Membrane Development**

The primary focus of this task was to translate the planar and spiral-wound composite membrane fabrication technology to the commercially viable form of a multilayer composite hollow fiber membrane. For this purpose, laboratory modules were to be fabricated and evaluated as a function of several process variables including total gas pressure, acid gas partial pressure, temperature, and feed and permeate gas water vapor content. A second aspect of this task was to provide (a) feedback to substrate development efforts to help define support fiber parameters such as base permeance, pore size, and porosity, etc. and (b) feedback to process application development efforts to gauge the effectiveness of ATMs in natural gas applications.

- **Process Application Development and Economic Analysis**

Efforts were to focus on defining new gas processing schemes centered on ATMs and/or on hybrids of ATM and current acid gas removal (AGR) technology. Optimization of the process would define the bottom line economic and energy savings benefits of the ATM process as compared to other membrane systems and other stand-alone gas processing technologies. Results from these studies would guide laboratory work in both substrate development and composite membrane development.

The results of this program are described in the following chapters.

III. Substrate Fiber Development

The goal of this task is to develop a high performance hollow fiber substrate to accept the active transport membrane coating and involves two major objectives: 1) identifying a polymer that fulfills the requirements of a "high performance" substrate and 2) developing spinning technology; that is, both the fiber spinning process and the polymer formulation needed to fabricate the identified polymer into a microporous hollow fiber substrate for suitable coating.

1.0 Introduction

Membrane devices can be fabricated as flat disks, plate and frame assemblies, spiral-wound elements and as hollow fibers. It is generally accepted that the hollow fiber module configuration has several advantages over other fabrication geometries including 1) hollow fibers are self supporting within a permeator thus allowing for a much simpler module fabrication process, and 2) hollow fibers generate higher surface area to permeator volume ratios than other configurations. These two factors suggest that the hollow fiber configuration should result in a significant reduction in cost over competing membrane technology.

Hollow fibers have been manufactured in the textile industry for the past several decades, mainly for use in thermal insulation applications. These fibers are typically produced by a melt-spinning process which involves heating a polymer above its melting point. The molten polymer is extruded through a spinneret to produce a fine filament which cools and solidifies into a fiber. The fiber produced through this method is dense across the entire wall of the fiber; that is, it contains no porosity. However, to produce the kind of the porous structure suitable for gas separation, a dry jet-wet spinning process (solution spinning) is commonly practiced. The dry jet-wet spinning process involves a phase inversion mechanism in which polymer solution is extruded as a fine tubular casting. The process can best be understood by considering the four steps of membrane formation: 1) extrusion, 2) air exposure/partial phase separation, 3) coagulation, and 4) washing/annealing. The reader is also referred to Figure 3-1.

- 1) **Extrusion:** A hollow fiber membrane is formed by extruding a concentrated polymer solution downward through a tube-in-orifice die (spinneret). The lumen (bore) of the fiber is created by delivering a coagulant fluid to the concentrically aligned capillary tube within the orifice. The extrusion results in a self supporting nascent hollow fiber.
- 2) **Air exposure/partial phase separation:** After extrusion, the nascent fiber travels through a short conditioning zone ("air gap") before entering a coagulation bath. In this stage, the polymer solution often undergoes a partial phase separation due to partial evaporation of the solvent, penetration of the ambient moisture into the extrudate, and/or temperature gradients established during the journey. Conditions in this critical zone can significantly influence membrane structure, especially the surface of the fiber, and were examined as part of this program.
- 3) **Coagulation/phase separation*:** Solidification of the fiber occurs by phase inversion (non-solvent induced phase separation) in the coagulation bath. In this stage, the polymer solution undergoes a more complete phase separation which results in a polymer-rich phase and a solvent-rich phase. This step plays an important role in determining the overall membrane structure especially that just under the surface layer. The effect of coagulation bath temperature on fiber properties was examined as part of this project.
- 4) **Washing/Annealing:** A water-wash step is employed to remove traces of residual solvent so that the pore structure created during the previous steps can be preserved. By this stage, morphology of the fiber has been determined, however, minor tuning in the pore structure may be achieved by warm-water annealing. The warm water washing can also enhance the rate of solvent exchange.

In the Phase I of this project, hollow fiber substrates were developed via the dry jet-wet spinning technique in the Corporate Science & Technology Center of APCI. The major task elements included setting support fiber criteria, identifying and evaluating candidate polymers against these criteria, studying candidate polymer processability for spinning, and initiating optimization of the spinning process and dope formulation for the polymer. Phase I goals included:

*A detailed description of the phase separation process can be found in *J.M.Sci.* (8), p. 41-57 (1993).

- to set-up a spinning line with controllable spinning parameters.
- to identify a spinnable polymer that fulfills the requirements for a composite membrane support for the targeted application.
- to gain an understanding of the operation variables-fiber property relationship.
- to develop reliable techniques to characterize the spun fibers.

2.0 *Experimental*

2.1 Hollow Fiber Spinning

A state-of-the-art hollow fiber spinning line was set up for this project. A schematic of the spinning line is shown in Figure 3-1. The major components of the line include: an in-line mixing system, a dope delivery system, a bore-fluid injection system, a coagulation bath, two duo-godet-wash bath assemblies, and a take-up winder.

- 1) *In-line mixing system:* The polymer solution (referred to as the "dope") was prepared in a customized Ross mixing system. The mixed dope can be transferred directly into the dope reservoir by a gear pump. In addition, degassing could be conducted inside the mixer by means of house vacuum. A condenser (heat exchanger) was attached to prevent solvent loss and maintain initial dope concentration.
- 2) *Dope Delivery System:* The resulting degassed dope solution was transferred from the reservoir to the spinneret via the gear pump. Before arrival at the spinneret the polymer solution was forced through a filter (mesh size: 60 μm) to remove particulates. The temperature of the entire delivery system was controlled using silicone rubber encased resistance heaters.
- 3) *Bore Fluid Injection System:* The internal coagulant (bore fluid) was supplied to the injection capillary of the spinneret via a bore fluid injection system. This set-up was designed to pump a small volume of fluid with a minimum of pulsing. The typical dope delivery pressure was about 3 psig.
- 4) *Coagulation Bath & Duo-godet-Wash Bath Assembly:* After extrusion, the partially solidified fiber was guided through a coagulation bath by a pair of

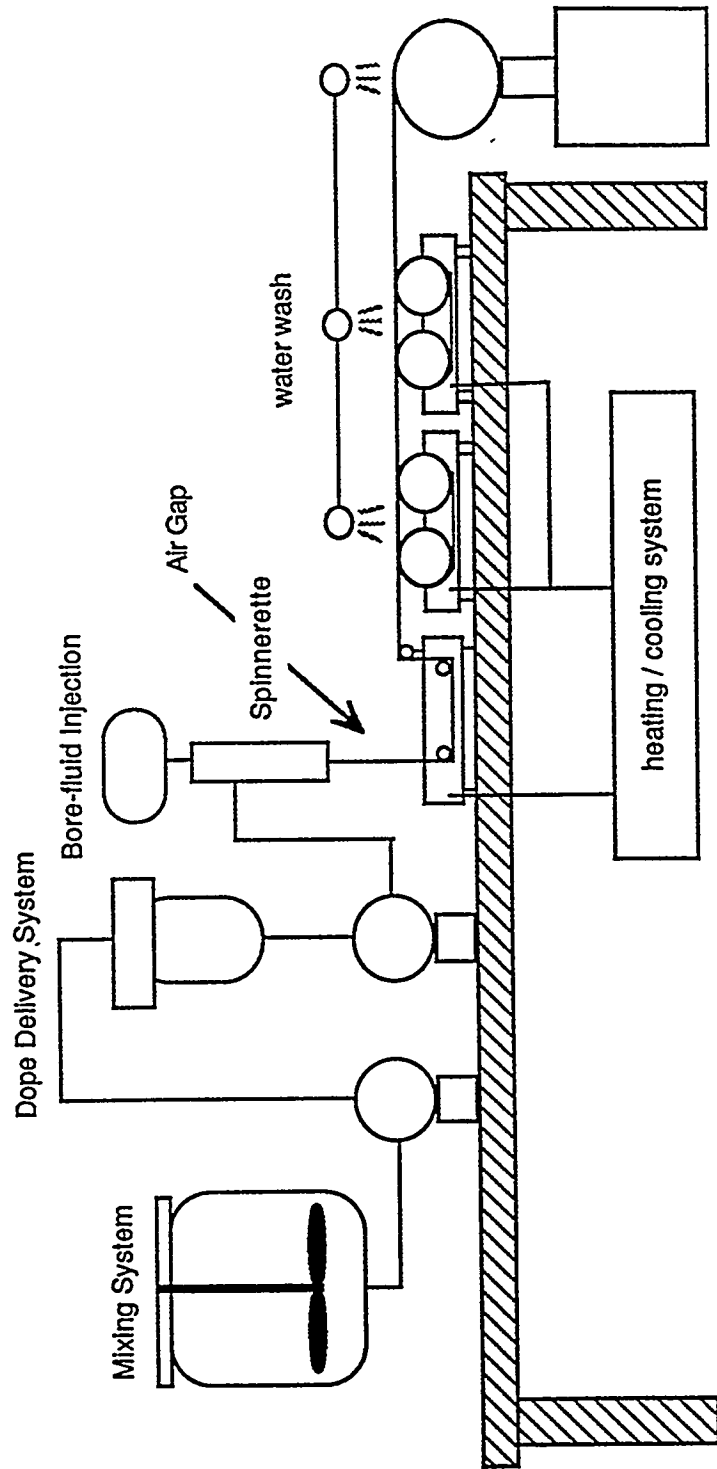


*Figure 3-1
Fiber Spin Line Schematic*

non-slip rollers (a duo-godet). On leaving the coagulation bath, the fiber was washed by entering a series of duo-godet-wash bath assemblies. The temperatures of the coagulation bath and wash baths, depending on experimental needs, were controlled by a circulating water bath.

- 5) *Take-up Winder and Fiber Storage:* After washing the fiber was wound onto a spool by an automatic, tension controlled take-up winder. Additional washing was provided at the winder by employing a water sprayer. The spooled fiber was stored in a water tank for at least 72 hours to remove the residual solvent which might be trapped in the fiber.

2.2 Hollow fiber Characterization

A typical spin run produced 1000-2000 linear feet of hollow fiber support membrane. Five foot lengths of fiber were cut from the spool and hung to dry at room temperature.

Characterization of hollow fiber support membranes included determining the overall fiber appearance, fiber dimension (outer diameter OD and inner diameter ID), average surface pore and defect size by optical and electron microscopy; quantifying the defect rate by bubble point measurements; measuring tensile strength by dynamic mechanical analysis; and measurements of gas permeance.

3.0 Result and Discussions

3.1 Polymer Selection Criteria and Candidate Polymer Screening

In order to qualify as a high performance acid gas substrate the candidate polymer should meet the following criteria: 1) good hydrocarbon resistance, 2) stable at end use temperature, 3) easily processable, and 4) commercially available. Polyimide-based polymers including PYLE-ML (polyimide), AI-10 (polyamide-imide), and PAI (polyamide-imide) were identified from the literature as potential support polymers.

The candidate polymers were first screened for processability, i.e. how easily could they be spun into hollow fibers. Table 3-1 summarizes the results of this investigation. High molecular weight (MW) PAI had the best processability among the polymers studied.

Table 3-1
Comparison in Spinning Processability

<u>Material</u>	<u>Source</u>	<u>Processability</u>
PYLE-ML	DuPont	fair
AI-10	Amoco	poor
AI-10	Air Products	poor
PAI (low MW)	Amoco	poor
PAI (high MW)	Amoco	good

Other critical properties were also examined. Table 3-2 lists physical properties of four commercially available polymers. Of the candidate polymers, PAI has the advantage of high temperature endurance as manifested by its high glass transition temperature (T_g) and superior mechanical strength as manifested by its high tensile strength. In addition, PAI shows the best hydrocarbon resistance. Table 3-3 shows the % tensile strength retained after 24 hour solvent exposure at 93°F. Commercial polymers such as polysulfone are degraded in, e.g., xylene and toluene. These investigations indicate that high molecular weight PAI is the most promising candidate among the polymers studied .

Table 3-2
Physical Properties of Candidate Polymers

<u>Properties</u>	<u>Udel</u> (3500) <u>Amoco</u>	<u>PAN</u> (PAN-X) <u>Bayer</u>	<u>Ultem</u> (1000) <u>GE</u>	<u>PAI</u> (4000) <u>Amoco</u>
MW	80,000	57,000	30,000	30,000
T _g (°C)	185	85	215	279
Tensile Strength (MPa)	70.3	118	105	135

Table 3-3
Hydrocarbon Resistance of PAI

<u>Chemical</u>	<u>% Tensile Strength Retained*</u>
Cyclohexane	100
Diesel Fuel	99
Gasoline (120 °F)	100
Heptane	100
Mineral Oil	100
Motor Oil	100
Xylene	100
Toluene	100

*After 24 hour exposure at 93 °C

Of the polymers investigated, PAI is clearly the leading candidate for further development. In addition to the general polymer criteria discussed above, other targets imposed on substrate fiber include:

- *good hydrocarbon/solvent resistance:* Screening studies measured hydrocarbon resistance of the bulk polymer. It is critical that this resistance be maintained after the polymer is spun into a fiber, especially in regard to those compounds present in natural gas streams.
- *good tensile strength:* The mechanical strength of the spun fiber should be strong enough for routine handling. The targeted tensile strength is comparable to that of commercial polysulfone fiber.
- *high gas permeance:* The initial base permeance for the support fiber is targeted at $\approx 1,000 \times 10^{-6} \text{ cm}^3/\text{cm}^2 \cdot \text{sec} \cdot \text{cmHg}$. However, the final flux target will be modified when it is integrated with the overall ATM performance targets set during composite optimization.
- *small and uniform surface pores:* Based on the molecular weight and radius of gyration of the ATM coating polymers, the target surface pore size is 100-200 μm .

However, the final target may vary with the chosen coating process and the coating material used.

- *compatibility with the ATM material.* The support fiber should be stable to ATM coating solvents (methanol and water). It should be wet by the ATM material and the resulting ATM-coated fiber should exhibit permselectivity close to intrinsic values.

The following sections of this chapter describe progress against these targets. It should be noted that these PAI fibers were developed throughout Phase I of this project and only limited work was performed to optimize substrate properties. Nonetheless, the results to date are encouraging. Support fiber optimization will continue as part of Phase II.

3.2 Solvent Resistance of PAI Support Fiber

In this study, the solvent resistance of polysulfone, Ultem, and polyacrylonitrile fiber was compared to PAI fiber. All fiber was produced by Air Products for this study.

The solvent resistance tests were performed by immersing small sections (5 cm) of fibers into five different solvents for a period of 2 weeks. The changes in fiber appearance were then observed and recorded. The solvents studied included 1,4 dioxane, 1,2 dichloroethane (DCE), tetrahydrofuran (THF), toluene, and hexane. These solvents are either common contaminants in streams or used for dissolving traditional coating polymers. Hexane is often a solvent used for dissolving polydimethylsiloxane (PDMS); the formulation is used to repair defective or leaky fibers.³¹ Table 3-4 summarizes the experimental results. All the fibers had good solvent resistance against the hexane. However, only the PAI fiber remained opaque in the other solvents studied. PAN fiber turned translucent and the others dissolved completely. The translucence of the fiber may indicate that solvent penetrates into the fiber wall, which may result in swelling. This study demonstrated that PAI fiber has the best solvent resistance among the examined hollow fibers. The order of solvent resistance of the fibers is: PAI > PAN > Ultem > polysulfone.

³¹ J.M. Henis and M.K. tripodi, Multicomponent Membranes for Gas Separations", U.S. Pat. No. 4,230,463 (1980).

Table 3-4
Chemical Resistances of Candidate Fibers*

Solvent	PSN	Ultem	PAN	PAI
Toluene	-	-	+	+
Dioxane	-	-	+	+
1,2 DCE	-	-	+	+
THF	-	-	+	+
Hexane	+	+	+	+

+ = stable; - = unstable

*After 2 week immersion at room temperature.

A more intensive test of PAI solvent resistance was also performed. The N₂ permanence of the support fiber was measured before and after exposure to the various solvents. Permeance loss (or gain) would indicate fiber degradation or changes to the micropore structure brought about by solvent exposure. The fiber used in this study had an initial permeance of 10,000 x10⁻⁶ cm³/cm²•s•cmHg. Small sections of fiber were immersed in the various solvents for 5 seconds. The permeance of the fibers was then remeasured and compared to the original values. Table 3-5 lists the percent permeance loss after solvent exposure. The permeance of PAI fiber is affected only by 1,2 DCE and methanol (40 % loss).

We have found that PAI solvent resistance can be improved by heat-treating the fiber at high temperature (over 200 °C) for several hours in an inert gas environment. This effect is also shown in Table 3-5. After thermal treatment PAI fiber had good solvent resistance even to DCE and methanol.

Table 3-5
Effect of Solvent Exposure on PAI Fiber Permeance

<u>Solvent</u>	<u>Permeance loss*</u>	
	<u>non-heat-treated</u>	<u>heat treated</u>
1,2 DCE	~ 40%	0%
MeOH	~ 40%	0%
Toluene	0%	0%
Hexane	0%	0%
Freon	0%	0%
Water	0%	0%

* after 5 sec solvent exposure

The necessity of the thermal-treatment process will be evaluated as part of Phase II. If this process is indeed needed, optimal curing time and temperature will be determined.

3.3 Tensile Strength of PAI Fiber

Tensile strength tests were performed to compare the PAI fibers with polysulfone, Ultem, and polyacrylonitrile (PAN) fibers. In addition, two types, microporous and asymmetric, of PAI fibers were compared. The results are shown in Table 3-6. PAI fiber has tensile strength comparable to other available fibers. In addition, the tensile strength of the PAI fiber depends on the fiber microstructure (asymmetric vs. microporous). The strongest PAI fiber produced so far has a tensile strength of 43% greater than polysulfone, and 150% greater than PAN. Overall, the PAI fiber has better mechanical strength (higher tensile strength) but less elasticity (lower elongation %) than the polysulfone and PAN fibers.

Table 3-6
Tensile Strength Tests of Fibers

<u>Hollow Fiber</u>	<u>Structure</u>	<u>Tensile Strength at Break*</u>	<u>Elongation at Break*</u>
Polysulfone	asymmetric	1.0	1.0
PAN	microporous	0.56	0.83
Ultem	microporous	0.92	0.29
PAI	microporous	1.43	0.39
PAI	asymmetric	1.12	0.88

* polysulfone = 1.0

The tensile strength of the fiber may depend not only on the material itself but also on the fabrication process and the dope composition. These factors could result in significant variations in fiber porosity, pore size, pore size distribution, phase separation mechanism (e.g. spinodal decomposition vs. nucleation and growth), and the existence of macrovoids. It should be noted here that the polysulfone fibers were spun from a higher polymer content dope than PAI and this may influence the results. Nonetheless, microporous PAI fibers were found to have the highest tensile strength among all the fibers investigated. Further improvement in fiber tensile strength and elongation % may be achieved through substrate optimization.

3.4 Pore Size/Permeance Control of PAI Substrate

Two important issues in developing the hollow fiber substrate are matching the support fiber properties to the needs of the coating polymer and ensuring that fiber manufacturing techniques will consistently produce uniform, high performance substrate. The ability to control the surface characteristics (e.g. pore size, porosity, and permeance) of the fiber is critical in matching the support fiber to the properties of the coating polymer. In addition, the ability to understand the effect of process variables on fiber properties is vital to ensuring fiber reproducibility not just within a given spinning run but also between spinning runs.

Fiber spinning is a complex process involving many interdependent parameters. Our efforts focused on the effect of three process variables on fiber permeance and surface pore size. The air gap length, coagulation bath temperature, and the environment within the air gap, on fiber properties (permeance and surface pore size) were investigated. Details of the study are described in the following sections.

3.4.1 Effect of Air Gap Length on PAI Fiber

The air gap is the distance from the bottom of the spinneret to the surface of coagulation bath. Two processes can occur as the fiber traverses this distance: 1) thermal phase separation induced by the difference between spin dope temperature and ambient temperature and 2) solvent induced phase separation resulting from ambient humidity and/or vapors given off from the coagulation bath. The degree to which each process occurs (or whether it will occur at all) is in part determined by air gap length. Therefore, the effect of the air gap was measured while all other spin variables were held constant. In addition, since water was used in the coagulation bath, two coagulation bath temperatures, 70 and 10 °C were chosen in the study to provide some indication of the effect of "uncontrolled" humidity on fiber performance. The results, summarized in Table 3-7, indicate that both the gas permeance and surface pore size increase with decreasing air gap for a 70°C bath but that these parameters are not sensitive to air gap length at the lower bath temperature. Additionally, a dense skin was observed on the fibers for all three air gap lengths investigated at using a 10°C bath. This last result was confirmed by the very low (2-50 $10^{-6} \text{cm}^3/\text{cm}^2 \cdot \text{s} \cdot \text{cmHg}$) gas permeance of the fibers.

*Table 3-7
Effect of Air Gap on Fiber Permeance*

<u>Air Gap</u>	<u>70 °C Bath Temperature</u>		<u>10°C Bath Temperature</u>	
	<u>Permeance*</u>	<u>Pore Size</u>	<u>Permeance*</u>	<u>Pore Size</u>
30 cm	1500	200 Å	2	<40 Å
20 cm	6500	400 Å	52	<40 Å
10 cm	15000	1000 Å	33	40 Å

* $10^{-6} \text{cm}^3/\text{cm}^2 \cdot \text{s} \cdot \text{cmHg}$; average of at least 5 modules.

3.4.2 Effect of Coagulation Bath Temperature on PAI Fiber

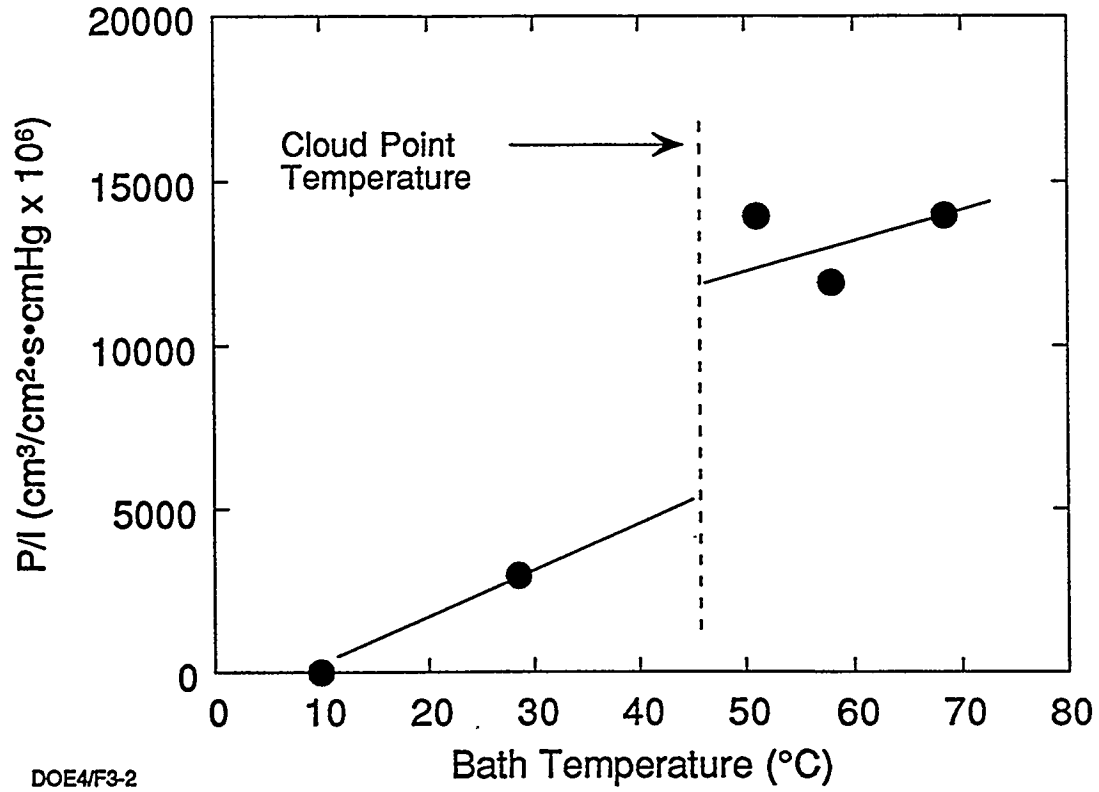
Coagulation bath temperature was varied from 10 °C to 70 °C while the other spinning parameters, including air gap length were held constant. Figure 3-2 shows the effect of coagulation bath temperature on fiber permeance. Higher coagulation bath temperatures resulted in a higher permeance substrate. As expected, the surface pore size of the fibers (~100 Å to ~1000 Å) increased with increasing coagulation bath temperature. The most permeable fiber was produced in a 70°C coagulation bath temperature of 70 °C and exhibited a permeance of $15,000 \times 10^{-6} \text{cm}^3/\text{cm}^2 \cdot \text{s} \cdot \text{cmHg}$ with a surface pore size of ~ 1000 Å.

3.4.3 Effect of Environment Within the Air Gap on PAI Fiber

As suggested in Table 3-7, the environment within the air gap can have a profound effect on the fiber properties. The aim of this study was to examine the extent to which the surface pore size and morphology could be controlled by maintaining a specific set of conditions within the air gap. The influence of the coagulation bath temperature (coagulation bath media vapor pressure) on the environmental effect within the air gap was also studied. Two coagulation bath temperatures, 51°C and 60 °C, were used in this investigation.

A "chimney" enclosing the spun nascent fiber within the air gap area was designed and installed to better control the environment within the air gap. An opening at the bottom of the chimney served as the inlet for the flowing gas which was vented at the top of the chimney. The experiments were conducted to compare the difference in fiber properties

Figure 3-2
Effect of Coagulation Bath Temperature on Permeance



between environmental and non-environmental control of the air gap. The air gap environment was changed by flowing, countercurrent to the fiber, dry nitrogen at 400bsccm. In the "no control" case, the chimney was in place but no gas was flowing.

Table 3-8 lists the resulting fiber permeances and surface pore sizes for the fibers. Interestingly, significant differences in both the permeance and the surface pore size between the fibers produced with and without the environmental control were observed. It should be noted that a more porous structure was produced in the non-environmental control condition.

Table 3-8
Environmental Effect in Air Gap on Fiber Property
(Coagulation Bath Temperature 51 °C)

<u>condition</u>	<u>P/l N₂*</u>	<u>surface pore size</u>
dry N ₂	5	dense (< 40 Å)
no control (56%)	4910	~100Å

* 10⁻⁶ cm³/cm²•s•cmHg

In the second set of experiments, the coagulation bath temperature was set at 60 °C. In the first data set, the air gap contained flowing dry N₂. In the second, the air gap contained nitrogen humidified to a dew point of 70C. In the last set, no gas was flowing. Table 3-9 compares the results for fibers spun under these conditions. A low permeance fiber was obtained with dry nitrogen circulating through the chimney. The general trend of this result is consistent with that obtained in the lower coagulation bath temperature. It is believed that dry N₂ both lowers the effective water (bath) vapor pressure and accelerates the rate of evaporation, leading to a less porous surface. A fiber with an extremely high permeance, moderate surface pore size, and high porosity (20%) was produced when warm, moist N₂ filled the air gap. It is believed that this condition should enhance a uniform phase separation through the cross-section of the nascent spun fiber (the fiber just extruded from the spinneret). Fiber produced without environmental control has a high permeance and large surface pores but a low porosity (7%). In addition, no macrovoids* were observed for the fibers produced with the environmental control while some macrovoids were observed in the non-environmental control condition.

*Large areas of free volume within the fiber wall

Table 3-9
Environmental Effect in Air Gap on Fiber Property
(Coagulation Bath Temperature 60 °C)

<u>control condition</u>	<u>P/l*</u>	<u>macrovoid</u>	<u>pore size</u>
dry N ₂	129	no	~ 100 Å
warm wet N ₂	97300	no	~ 800 Å
no control**	67080	yes	~ 500 Å

* $10^{-6} \text{ cm}^3/\text{cm}^2 \cdot \text{s} \cdot \text{cmHg}$

** ≈60% relative humidity

4.0 Summary and Recommendations

In Phase I of this project, a state-of-the-art spinning line was designed, installed and used to examine the relationship between various parameters in the spinning process. This line was set up to simulate a continuous manufacturing process from polymer formulation to fiber formation and winding. A set of routine characterization methods were developed to examine the quality of the spun fibers including permselectivity measurements, surface pore size, defect pore size and rate, solvent resistance, and tensile strength.

A polymer fulfilling the substrate requirements was identified. A dope formulation and spinning process for this material were demonstrated. A parametric study identified key parameters for controlling surface pore size and fiber permeance. Fiber permeance and surface pore size were found to be strong functions of the air gap length, coagulation bath temperature, and the environment within the air gap. Circulating dry nitrogen through the air gap produces fiber with smaller surface pores while warm and wet nitrogen within the air gap produces fiber with large surface pores and high porosities. The nonoptimized fiber has met the preliminary targets set for a high performance substrate and shows promise as a coatable substrate for the ATM material. The current status of fiber development is summarized in Table 3-10.

Table 3-10
Current Status of Development

<u>Parameter</u>	<u>Status</u>
High Gas Permeance	up to 100,000 $10^{-6}\text{cm}^3/\text{cm}^2\cdot\text{s}\cdot\text{cmHg}$
Small Surface Pores	tunable from < 40 to 1000 \AA
Tensile Strength	comparable to commercial fiber
Hydrocarbon Resistance	Good

A follow-on program should focus on optimizing the PAI hollow fiber by incorporating results from ATM coating studies. The spinning process is complex and its variables are often interdependent. Therefore, a forward program should include the completion of a process variables / fiber property relationship matrix. An optimal dope composition and process conditions for scale-up should be determined. Finally, fibers with the desired properties should be produced in large quantity to support laboratory module fabrication and field testing efforts. The necessity of the post-spinning thermal treatment should also be examined during that segment.

IV. Composite Membrane Development

The objective of this task was to demonstrate the separation of CO₂ from CH₄ using hollow fiber active transport membranes. This objective was met by forming thin film composite membranes of the AT polyelectrolyte PVBTAF and polysulfone or PAI hollow fiber substrates. Lab-scale modules were evaluated at pressures up to 900 psi and for periods as long as 1 month. This chapter is divided into three sections. The first describes the characterization of the candidate coating solutions in terms of their solubility, viscosity, molecular weights, etc. The second reports on the coatability of potential substrate materials with PVBTAF by fabricating and evaluating planar thin film composite membranes. The last describes the fabrication and evaluation of lab-scale hollow fiber modules.

1.0 Physical Properties of Coating Solutions

1.1 Molecular Weight and Distribution of ATM Polymers

Most coating work employed the AT polymer poly(vinylbenzyltrimethylammonium fluoride), PVBTAF. This polymer is derived from either of two batches (batch 1 and batch 2) of poly(vinylbenzyltrimethylammonium chloride), PVBTACl³² which differed in molecular weight. Molecular weight, molecular weight distribution and estimated molecular size were determined using Gel Permeation Chromatography/Magic Angle Laser Light Scattering (GPC-MALLS). Results are shown in Table 4-1. The molecular weight of all samples were sufficiently high ($M_w > 500,000$) to be film forming. The radius of gyration, an estimate of the volume occupied by a polymer chain in solution, is 400-500 Å suggesting that a substrate fiber with surface pores smaller than 1000 Å diameter will be required. Other work focused on coating substrates with poly(diallyldimethylammonium fluoride), DADMAF, and proprietary blends based on high molecular weight poly(vinylalcohol), PVOH ($M_w > 100,000$). These polymers were also film forming and of similar radius of gyration.

³²Details of the synthesis of AT polyelectrolytes can be found in U.S. Pat. No. 5,336,298

Table 4-1:
GPC MALLS Molecular Weight Determination of
Poly(vinylbenzyltrimethylammonium) and
Poly(diallyldimethylammonium) AT Polymers

<u>Reference</u>	<u>Sample</u>	<u>Batch No.</u>	<u>Mw</u>	<u>Mw/Mn</u>	<u>Rg (Å)</u>
13100-17-1	PVBTACI	1	739,000	2.5	463
13371-4A	PVBTAf	1	822,000	3.0	445
13771-4B	PVBTAf	1	841,000	3.0	444
13649-14A	PVBTACI	2	1,270,000	2.5	486
13391-34-2	PVBTAf	2	1,129,000	2.1	461
13100-12-1	DADMACI	1	239,000	4.6	312
13100-13-1	DADMAf	1	343,000	6.8	343

1.2 Solubility of AT Polymers

All the Active Transport polymers are soluble in water to at least 15 wt% polymer. PVBTAf and DADMAf are also soluble in methanol (MeOH) to at least 5 wt% polymer.

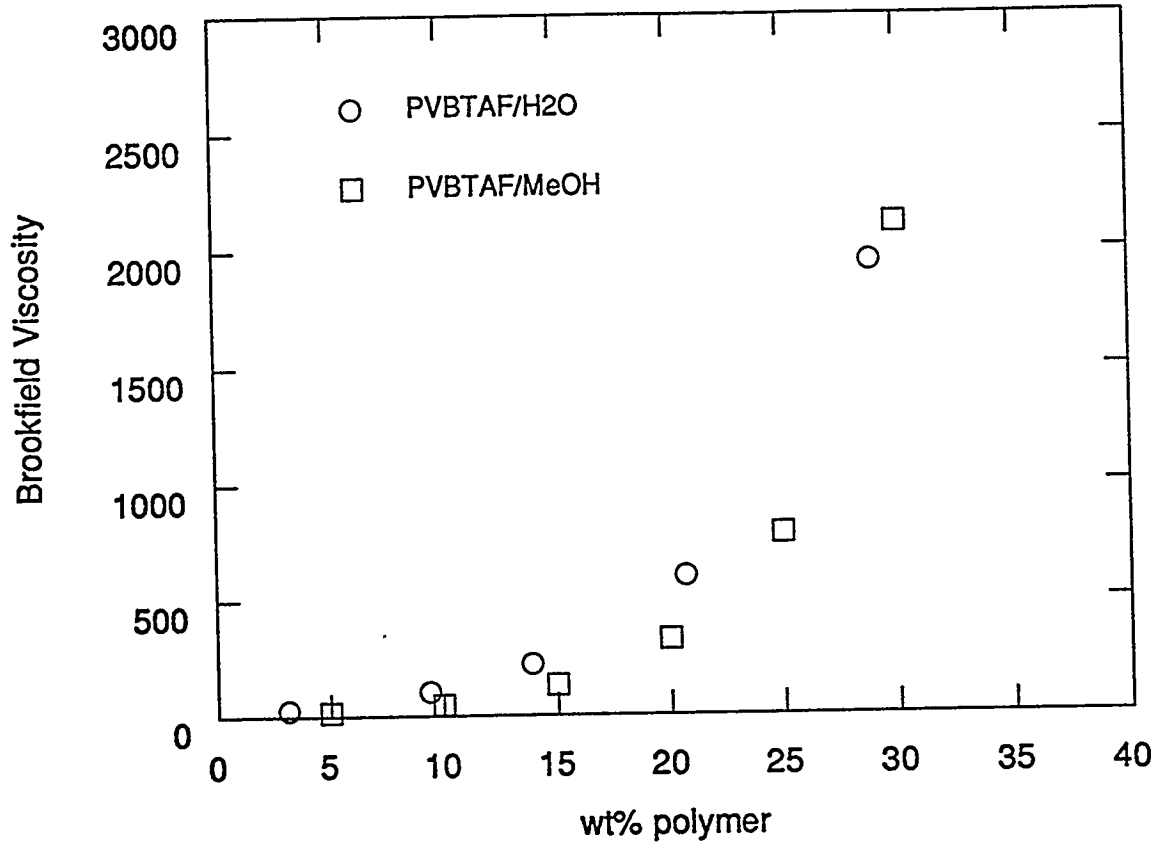
1.3 Viscosity of ATM Solutions

The room temperature viscosity of the primary ATM coating solutions (PVBATf/H₂O and PVBTAf/MeOH) was determined using a Brookfield Digital Viscometer. Viscosity was measured for polymer concentrations between 1-35 wt%. Solution viscosity is plotted in Figure 4-1. The measured viscosity is the same for the two solvents indicating that water and methanol are equally good solvents for PVBTAf.

1.4 Wetting Behavior of AT Systems

Wettability can be estimated by measuring the contact angle between the coating solution / solvent and the substrate. Wettability can be inferred if the contact angle is less than 90°.

Figure 4-1
Viscosity of ATM Coating Solutions



13095-98
13921-23
DOE4/F4-1

Conversely, the materials are nonwetting if the contact angle is substantially greater than 90°. Several methods for measuring contact angles are given in reference³³. This work employed two methods to measure the contact angles. In one, the contact angle between coating solvents and dense planar coupon of substrate was measured by the sessile drop technique. The results (Table 4-2) indicate that both solvents wet the substrate.

Table 4-2
Contact Angle of ATM Solvents with Substrate Polymers

<u>Substrate Polymer</u>	<u>Contact Angle</u>	
	<u>Water</u>	<u>Methanol</u>
polysulfone	≈ 60°	≈55°
PAI	≈50°	≈40°

The *dynamic* contact angle between PAI fibers and ATM solutions was examined by hanging a small section of the dense substrate fiber from a Cahn micro-balance and monitoring the weight change as a function of time while either dipping the fiber into the test solution (advancing angle) or pulling the fiber out of the solution(receding angle). A dense rather than microporous substrate was used to prevent wicking of the solution into the pore wall. The fiber end contacting the polymer solution was sealed in an epoxy resin to prevent capillary rise of the solution into the fiber bore. In this study, the solutions were 1 wt% PVBATF in water or in methanol. The surface tension of the ATM solutions was 70 and 23 dynes/cm, respectively - slightly lower from the pure solvent values of 72.6 and 24.0 dynes/cm. The dynamic contact angles were calculated from the surface tension of the solution, the surface area of the fiber, and the weight change upon contact with the solution.

Results are summarized in Table 4-3. Contact angles are less than 90 degree suggesting that PVBATF should coat PAI fiber. In reality a porous PAI substrate will be used. In that case the surface porosity of the substrate fiber should reduce the contact angle and therefore enhance the coatability.

³³A.W. Adamson, "Physical Chemistry of Surfaces"3rd ed., J. Wiley & Sons, New York (1976).

Table 4-3
Dynamic Contact Angle Between ATM Coating Solutions and PAI Fiber

<u>Contact angle</u>	<u>PVBTAf/H₂O</u>	<u>PVBTAf/MeOH</u>
Advancing	65.0°	50.0°
Receding	50.7°	44.5°

2.0 Coatability of Planar Substrate Coupons

The coatability of polysulfone and PAI with PVBTAf was investigated by fabricating small laboratory test coupons (flat sheet membranes about 2 inches in diameter) for screening studies. The microporous polysulfone support membrane was made by a proprietary process. Microporous PAI support membranes were produced via phase inversion technology using the spin dope formulations described in Chapter 3. Membranes were examined using optical or electron microscopy and were also evaluated for permselectivity. The surface pores of the uncoated PAI support ranged from 300Å to 1000Å in diameter; its N₂ permeance was $\geq 70 \times 10^{-6} \text{ cm}^3/\text{cm}^2 \cdot \text{s} \cdot \text{cmHg}$. The N₂ permeance of the planar polysulfone membrane was $\geq 100 \times 10^{-6} \text{ cm}^3/\text{cm}^2 \cdot \text{s} \cdot \text{cmHg}$. PVBTAf composite membranes were fabricated and evaluated as described previously²⁹. In general, adhesion between PVBTAf and the substrates was good, however, some delamination occurred at extremely low humidity ($P/P_0 < 0.05$). Representative screening results are shown in Tables 4-4 and 4-5.

Table 4-4 : Permselectivity of a PVBTAF/Polysulfone Flat Sheet Composite Membrane as a Function of CO₂ Pressure (12484-76B)

<u>Feed Pressure (psig)#</u>	<u>P_{CO₂} (cmHg)</u>	<u>P/I CO₂(x 10⁶)*</u>	<u>αCO₂/H₂</u>	<u>αCO₂/CH₄</u>
5.3	31.7	6.02	87	1024**
20.0	55.0	4.51	82	765**
40.0	86.7	3.78	71	640**
61.1	120.1	3.19	48	540**
75.6	143.1	2.88	43	490

feed mix: 30% CO₂/34% CH₄/36%H₂

Temp=23°C; P/P₀=0.31

* units of cm³/cm²•s•cmHg

** no CH₄ detected in permeate; selectivity estimated from observed CH₄ permeance at 75.6 psig

Table 4-5: Permselectivity of a PVBTAF/PAI Planar Coupon as a Function of CO₂ Pressure (12484-82)

<u>Reference</u>	<u>Feed Pressure (psig)#</u>	<u>P_{CO₂} (cmHg)</u>	<u>P/I CO₂ (x 10⁶) *</u>	<u>αCO₂/H₂</u>	<u>αCO₂/CH₄</u>
uncoated PAI #1	15	51	1030	1.2	1.0
PVBTAF-coated	39.7	93.2	1.38	48	>150**
	102.5	201	0.915	33	>100**
uncoated PAI #2	39.0	92.3	70	0.63	0.91
PVBTAF-coated	39.0	92.3	3.05	50	>300**
	99.0	196	0.804	10	>85**

feed mix: 33% CO₂/33% H₂/34%CH₄

Temp=23°C; P/P₀=0.31

* units of cm³/cm²•s•cmHg

**no CH₄ detected in permeate; selectivity estimated from detection limits of gas chromatograph

These results demonstrate that it is possible to coat both polysulfone and PAI flat sheets with PVBTAF and that good permselectivity can be achieved. The facilitated transport aspect of the membranes is maintained as evidenced by the pressure dependent nature of the permselectivity.

3.0 Hollow Fiber Module Fabrication and Evaluation

3.1 Dip Coating Procedures

Microporous and dense hollow fiber substrates were coated with ATM polyelectrolytes by dip coating techniques. Dip coating is a batch process which simulates the elementary steps of a continuous meniscus coating operation. The elements of the dip coating process are shown schematically in Figure 4-3. First, the bottom of the fiber was either heat sealed or pinched closed to prevent penetration of the coating solution into the bore and the fiber was immersed into the coating bath containing 0.5-10 wt% ATM polymer for ≈ 15 sec. Coating solution was deposited on the fiber as it was withdrawn from the bath at a constant rate. An equilibrium liquid film thickness was established which depended on the viscosity of the coating solution, the contact angle between the coating solution and the fiber, the surface tension of the liquid, the rate at which the fiber is drawn from the solution, and the fiber diameter. The coated fiber was hung to complete solvent evaporation and a dry coating was formed. Next an overcoat of a silicone rubber-like material (e.g. 1 wt% Sylgard 184 in isopentane or 1 wt% Petrarch PS254 in methylene chloride) was deposited by the same procedure. For comparison, a continuous coating process is shown in Figure 4-4. The coated fibers were stored at room temperature in a relative humidity of 20-40%.

The Deryaguin coating model, i.e. mathematical relationship between the various coating parameters described above, is shown in equation 1. This relationship is valid for nonporous substrates when the capillary number (Un/S) is in the range $10^{-5} - 10^{-2}$.^{34,35}

Equation 1:
$$h/R = 1.33 (Un/S)^{2/3}$$

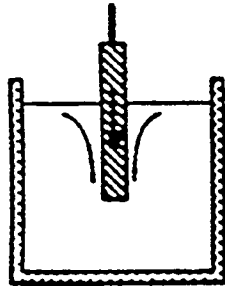
where h = liquid film coating thickness
R = fiber radius
U = fiber velocity
n = coating solution viscosity
S = surface tension of the coating liquid

Recently, Tsai et. al. have accounted for deviations from the Deryaguin model when microporous substrates are used. They postulated that capillary suction of solvent into the

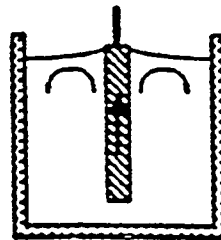
³⁴B.V. Deryaguin, *Acta Physicochim*, 20, 349 (1945).

³⁵D. Quere, J-M. Di Meglio and F. Brochard-Wyart, *Science*, 249, 1256 (1990).

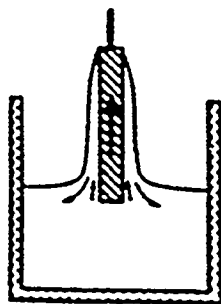
Figure 4-3
Schematic Representation of a Dip Coating Process



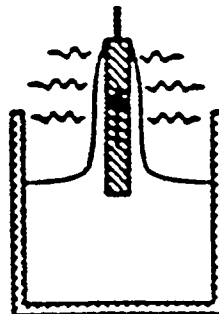
1) immersion



2) start up

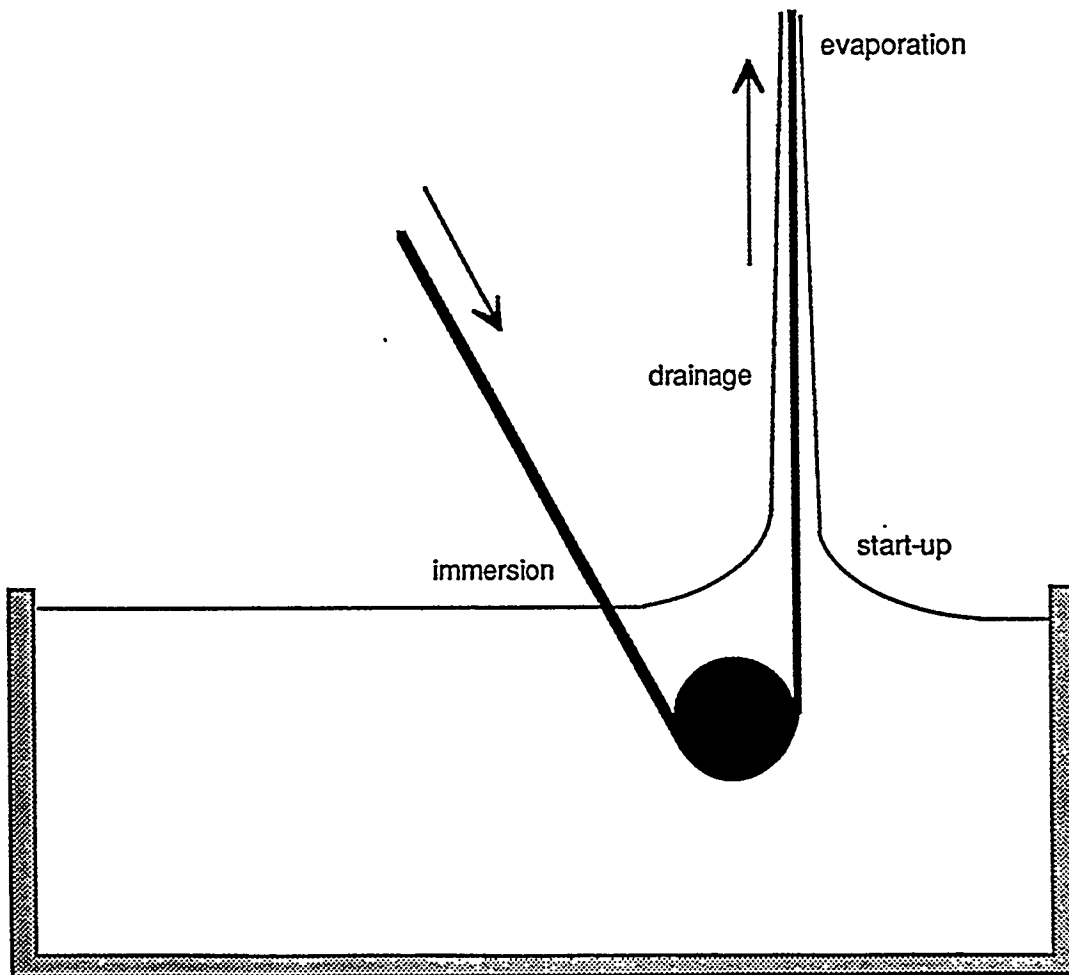


3) drainage



4) evaporation

Figure 4-4
Schematic representation of a Continuous Meniscus Coating Process



pores of substrates results in a localized viscosity increase near the fiber surface. Thus, the wet film thickness on microporous substrates is greater than if a nonporous substrate is used. This refined Deryaguin model requires knowledge of the equilibrium capacity and the kinetics of solvent absorption by the fiber.

The various support fibers used in this work were coated from aqueous or methanolic solutions containing 0.5 - 10 wt% Active Transport polymer. The ratio of wet film thickness to fiber radius (h/R), estimated from the Deryaguin model, ranged from 0.004 to 0.02. (There is currently insufficient information to apply the refined Deryaguin model.) Lab-scale modules, containing between 1 and 50 nine inch long fibers, were fabricated by potting a fiber bundle into a stainless steel housing as shown in Figure 4-5. Feed gas was circulated on the shell side. The active fiber length was nominally taken as 9" in all modules although small variations between modules were likely. In most experiments the bore, or fiber lumen, was swept with an inert gas (helium or nitrogen) in order to facilitate detection of the permeating species by a gas chromatograph. Details of the experimental procedures can be found in previous reports.^{28,29}

3.2 Results and Discussion - PVBTAF Coated Commercial Substrates

3.2.1 Membrane Characterization

Substrate Characterization

This phase of the work used two types of commercial polysulfone hollow fiber substrates which are here designated SUB1 and SUB2 (substrate 1 and substrate 2). Both fibers were asymmetric with a very thin dense skin on the shell-side of the fiber. The fibers differed in their wall and skin thickness. For example, the wall of SUB1 was approximately twice that of SUB2. It is important to note that neither fiber was optimized for use as a thin film composite substrate. In addition, the fibers were found to contain manufacturing flaws or defects which include small amounts of surface debris and gouges in the skin (Figures 4-6).

Characterization of the Composite Hollow Fiber Membrane

Scanning Electron Microscopy (SEM) was the primary characterization tool. The only procedure which produced a sharp cross-section was one in which the sample was frozen in liquid nitrogen and then gently fractured. However, the coatings of samples prepared even by this method often delaminated making it difficult to consistently obtain meaningful cross-

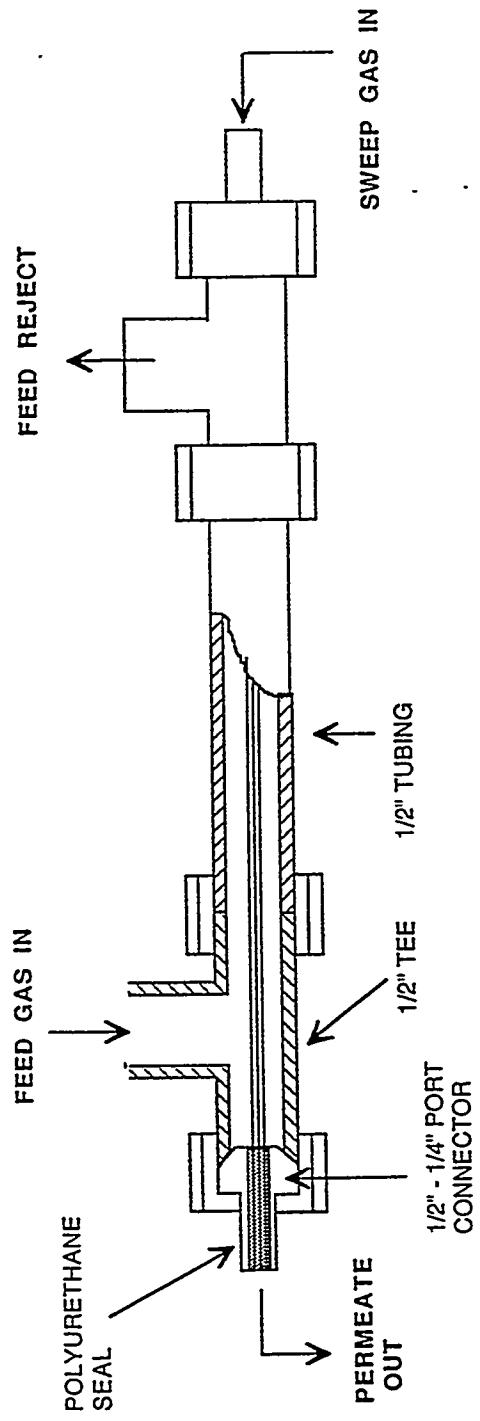
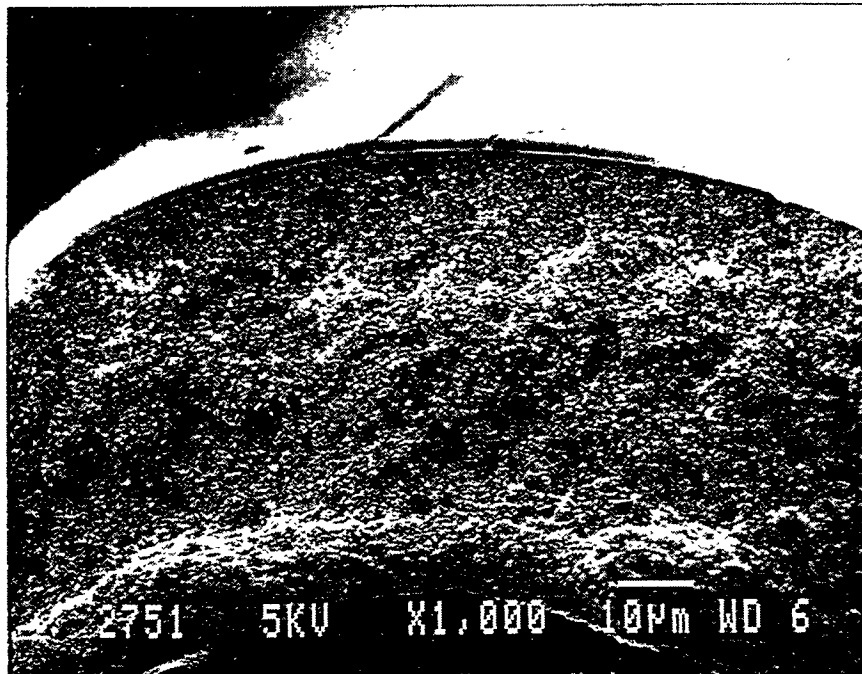


Figure 4-5
 Lab-Module Potting Arrangement

Figure 4-6
Apparent Manufacturing Defects of SUB1 and SUB2 Substrates



Figure 4-7
Representative Cross-section of ATM-coated SUB1



section analysis. The ATM layer was usually found to be between 2 and 10 μm thick (Figure 4-7).

3.2.2 Permselectivity Evaluation

Modules were evaluated for CO_2 , CH_4 and, in some cases, H_2 permselectivity in a mixed gas, flowing test system similar to those described earlier.²⁹ The water content of the feed and sweep gases as a critical experimental parameter³⁶. Therefore, the test system incorporated a means to vary the hydration level of the feed and sweep streams from $P/P_0 \approx 0.2$ to $P/P_0 \approx 0.8$ where, P is the H_2O vapor pressure at the hydrating bubbler temperature and P_0 is the vapor pressure of H_2O in equilibrium with liquid water at the temperature of the membrane. Chilled mirror hygrometers (General Eastern Corp.) were used to measure the dew point of the gas feed and permeate but it was not possible to obtain an accurate mass balance of H_2O by this method.

The permeance (P/ℓ) of the various components was calculated using the known or experimentally determined parameters from the equation:

$$(P/\ell)_i = F_i / A \cdot \Delta P_i$$

and the set of simultaneous linear equations:

$$[i] = F_i / \sum F_i$$

where

F_i = flow rate of permeating species i

A = membrane area, based on the OD of the uncoated substrate fiber

ΔP_i = partial pressure driving force of species $i = P_i$ (feed source) - P_i (bulk permeate)

$[i]$ = concentration of species i as determined by gas chromatography

$\sum F_i$ = total species flow rate in the N_2 -swept permeate stream

³⁶For a full discussion of this effect see Section V.1.0 of this report.

The calculated permeance is that of the module under the given set of experimental conditions. A model which would (1) derive the composite membrane properties from the experimentally determined module properties and also (2) derive the intrinsic AT layer properties from the composite properties does not exist at this time. This treatment of the data penalizes the module to some degree since experimental data was often taken under non-zero recovery of CO₂; that is, only 1-15% of the CO₂ in the feed gas was allowed to permeate the membrane. In most cases however, the membranes were operated under zero recovery of H₂O.

More than 40 PVBTAf-coated SUB1 and SUB2-based modules were fabricated and evaluated. A summary of results is provided in Table 4-6. Early attempts at fiber coating and module fabrication used SUB2 fiber and were not very successful. Eventually, modules utilizing both Sub1 and Sub2 were successfully fabricated and evaluated. Specific examples illustrating important concepts or results are detailed below.

- P/I CO₂ and $\alpha_{\text{CO}_2/\text{CH}_4}$ as a function of CO₂ Partial Pressure [13074-67C]

A commercial ATM will have to operate near natural gas well-head pressures (about 1000 psi). These conditions were simulated in the test equipment. The SUB1-based hollow fiber ATM was evaluated as a function of total feed gas pressure up to about 800 psig while the permeate pressure was maintained at approximately 15 psia. The results are shown in Figure 4-8. Because CO₂ is transported via a chemically-assisted pathway, its permeance is pressure dependent and is highest at low CO₂ feed partial pressures. Its value depends not solely on the partial pressure difference but on the specific value of the partial pressures^{3,28}. Methane is transported via a Henry's Law solution-diffusion pathway and hence, its permeance is independent of pressure. Thus, the $\alpha(\text{CO}_2/\text{CH}_4)$ also varies with CO₂ feed pressure. The most important conclusion from this study is that the composite hollow fiber module is dimensionally stable at high pressure. In the extreme, the transmembrane pressure was almost 800 psi. At high CO₂ partial pressure, where the chemically-assisted pathway is saturated, $\alpha(\text{CO}_2/\text{CH}_4)$ was ≈ 75 which is 3-4 times higher than the pure component selectivity of most polymer membranes at < 100 psig.

PVBTAf-coated SUB1 Fibers
 25% CO₂, 25% CH₄, 50% H₂ @ 75 sccm

Reference #	P/Po	cmHg CO ₂	P/LCO ₂	CO ₂ /CH ₄	I on Stream	Comments
13074-67C	0.27	69	2.98	366	13 days	
	0.27	156	1.87	200		
	0.27	291	1.12	147		
	0.27	416	0.929	126		
	0.27	544	0.757	111		
	0.27	681	0.629	91.5		
	0.27	806	0.549	84.5		
	0.27	949	0.463	76.1		
	0.27	1072	0.399	71.3		
	0.27	1105	0.480	73.3		
	0.27	699	0.609	87.6		
	0.27	348	1.111	146		
	0.27	153	1.60	201		
13074-88A	0.27	70	1.69	265		no sweep
	0.27	68	2.54	364		no sweep
	0.27	71	1.65	216		no sweep
	0.27	84	0.424	1.8		no sweep
	0.28	79	2.00	221	8 days	no sweep after H ₂ S testing
13399-40	0.28	143	1.55	135		20 sccm feed
	0.28	147	1.60	151		20 sccm feed
	0.28	541	0.669	48.2		
13399-41	0.28	815	0.505	32.9		
	0.34	96	3.493	108	4.5 days	
	0.24	93	2.702	134		
	0.49	93	4.445	57.6		
	0.34	96	3.829	134	5 days	
13399-41	0.24	96	2.735	202		
	0.17	92	1.871	252		
	0.23	92	2.300	257		

Table 4-6

Summary: Permselectivity of PVBTAf-coated SUB1 and SUB2 Modules

<u>Reference #</u>	<u>P/Po</u>	<u>cmHg_{CO2}</u>	<u>P/CO2</u>	<u>CO2/CH4</u>	<u>T on Stream</u>	<u>Comments</u>
13921-24 lifetime test	0.27	100	0.98	300	48 days	H2S-free (25% CO2 in CH4) 0.3% H2S, unstable 3% H2S H2S-free
	0.27	100	0.87	280		
	0.27	114	0.49	150		
	0.27	100	0.50	260		
13921-25	0.27	100	2.20	250	48 days	H2S-free (25% CO2 in CH4) 0.3% H2S, unstable 3% H2S H2S-free
	0.27	100	1.75	245		
	0.27	114	0.92	150		
	0.27	100	1.05	210		
13921-45	0.27	52	0.47	144		
	0.20	53	0.27	111		
	0.15	52	0.19	72		
13921-54	0.27	53	1.80	316	12 days	feed : 10% CO2 in CH4
	0.39	53	2.68	164		
	0.53	53	3.83	75		
	0.72	53	5.75	43		
	0.27	53	2.08	273		
	0.19	53	1.49	351		
	0.15	53	1.04	356		
	0.09	53	0.64	134		
0.27	53	2.04	212			

Table 4-6 (cont'd)

PVBTAf-Coated SUB2 Fibers
 (coatings are PDMS/PVBTAf unless otherwise stated)
 feed gas is generally 25%CO₂, 25%CH₄, 50% H₂

Reference #	P/Po	cmHg CO ₂	P/ICO ₂	CO ₂ /CH ₄	I on Stream	Comments
12577-97B	0.16 0.16	55 58	1237 85.0	0.9 1.0	1 day	no coating no PDMS
MOD I	0.18 0.38	61 59	809 8.03	0.9 28.3	1.5 days	no coating 2 PVBTAf dips/no PDMS
MOD III					0.5 days	potted in septa
MOD IV	0.34 0.34	57 58	6.89 6.29	22.5 18.2	1 day	potted in septa; PVBTAf only PVBTAf+PDMS
13074-1	0.36 0.36	59 59	18.3 5.91	1.7 22.3	2 days	PVBTAf repair
13074-3B	0.38 0.38 0.38	63 59 57	5.56 4.27 4.21	60.5 55.3 57.0	1.5 days	195 sccm feed
13074-3C	0.38 0.38 0.38 0.38	66 62 62 71	4.58 7.34 4.92 4.24	42.3 57.9 37.6 11.6	1.5 days	195 sccm feed
13074-13G	0.38 0.38	65 67	4.46 2.17	32.9 19.7	1 day	20 sccm feed
13074-17B	0.38 0.38 0.38	65 65 65	3.77 3.26 3.31	44.8 39.5 41.5	3.5 days	20 sccm feed
13074-23B	0.38	63	4.50	44.0	0.5 days	

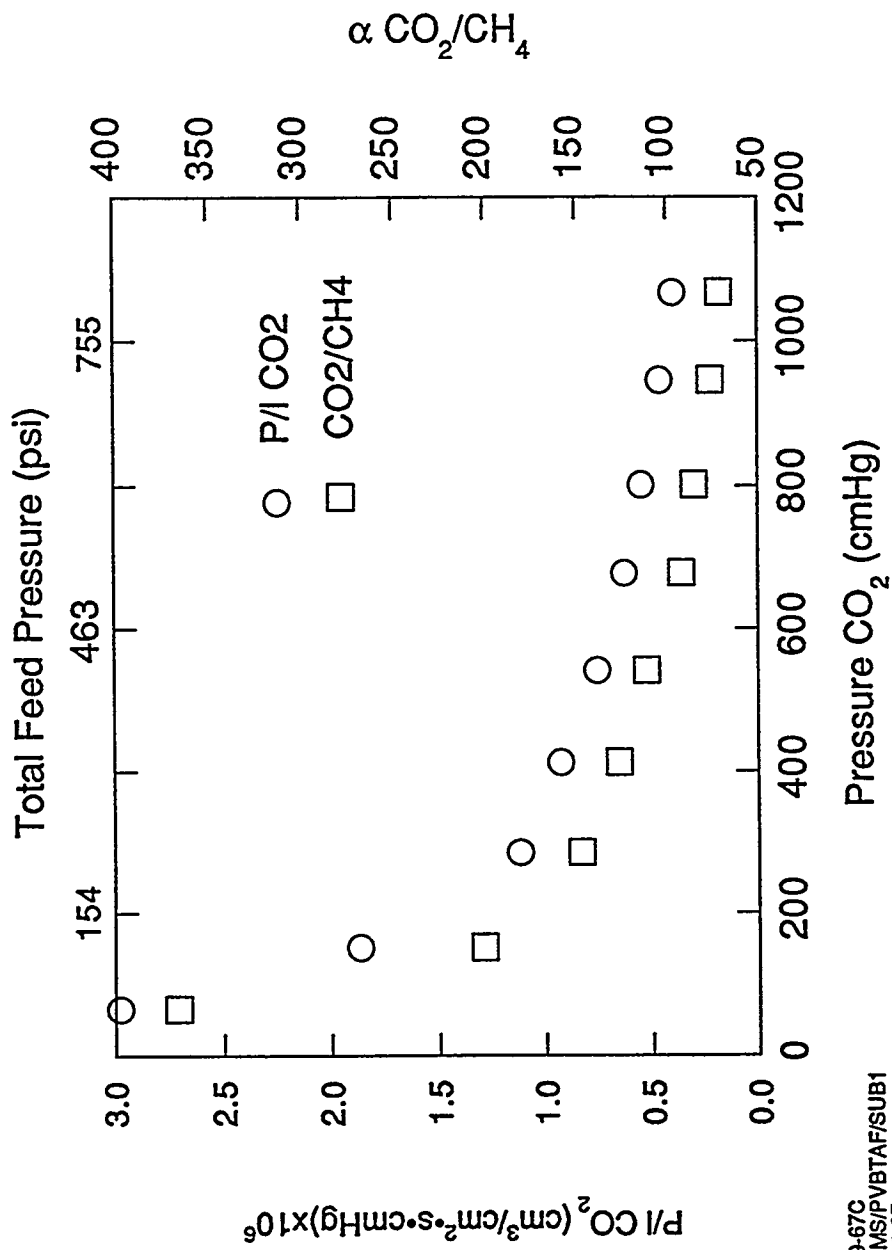
Table 4-6 (cont'd)

<u>Reference #</u>	<u>P/Po</u>	<u>cmHg CO2</u>	<u>P/CO2</u>	<u>CO2/CH4</u>	<u>I on Stream</u>	<u>Comments</u>
13074-23C	0.38	62	13.76	1.6	0.5 days	
13074-23D	0.38	62	206	1.0	0.5 days	
13074-23E	0.38 0.38	62 62	4.79 3.85	7.0 2.0	0.5 days	
13074-26B	0.38	62	3.37	14.3	0.5 days	13074-23D recoat
13074-29B	0.38	62	5.36	10.2	0.5 days	
13074-29C	0.38 0.38 0.38 0.27 0.27	65 65 65 65 65	4.78 4.29 4.63 3.45 3.27	200 315 226 78.4 276	2 days	20 sccm feed 20 sccm feed
13074-31B	0.38 0.38	62 62	4.23 14.0	3.4 1.5	0.5 days	13074-29C recoat
13074-35A	0.38 0.38	62 65	4.08 6.23	10.0 8.9	0.5 days	13074-35A recoat
13074-35C	0.38 0.38 0.52 0.38 0.27 0.27 0.38 0.38 0.27 0.27	62 62 62 62 62 95 97 98 67 150	3.74 3.41 5.88 3.55 2.75 2.30 3.13 2.72 0.0239 0.0103	235 238 60.4 223 289 366 179 210 --- ----	6 days	20 sccm feed 20 sccm feed 20 sccm feed 20 sccm feed 20 sccm feed 20 sccm feed retest after H2S exposure
13074-40C	0.38 0.38	63 65	2.37 2.15	37.3 36.7	1 day	5" fiber 5" fiber; 20 sccm feed
13074-42C	0.38	65	1.78 4.40	98.0 86.7	0.5 days	

Table 4-6 (cont'd)

Reference #	Pi/Po	cmHg CO2	Pi/CO2	CO2/CH4	T on Stream	Comments
13074-42D	0.38	65	1.22	30.9	0.5 days	
13074-43C	0.38	65	4.35	37.3	2 days	polyurethane fill to ends
	0.38	65	3.33	60.9		
	0.27	65	2.08	78.0		
13074-49D	0.38	63	5.96	194	15 days	
	0.27	63	4.43	512		
	0.27	95	3.69	316		
	0.27	135	3.05	275		
	0.27	180	2.50	240		
	0.27	214	2.20	219		
	0.27	215	2.11	221		
	0.24	215	1.76	243		
	0.24	215	1.76	251		
	0.24	180	1.98	309		
	0.24	137	2.35	400		
	0.24	92	2.97	577		
	0.24	68	2.91	574		
	0.27	65	3.42	460		
	0.31	65	3.86	328		
	0.38	65	5.22	222		
13074-51C	0.27	71	2.05	195	13 days	
	0.38	70	3.25	142		
	0.24	71	1.77	171		
	0.27	152	1.44	124		
	0.27	217	1.14	80.7		
	0.27	286	0.895	58.8		180 sscm feed
	0.27	418	0.773	47.0		
	0.27	418	0.687	42.1		
	0.27	555	0.584	33.2		
	0.27	570	0.541	32		20 sscm feed
	0.27	689	0.463	27		
	0.27	822	0.404	9.5		

Table 4-6 (cont'd)



13399-67C
 8XP/MS/PVBTAF/SUB1
 P/Po-0.27
 DOE4/4-8

Figure 4-8
 Effect of Feed Pressure on Performance

- Effect of Fiber Strength on Membrane Integrity [13074-51C]

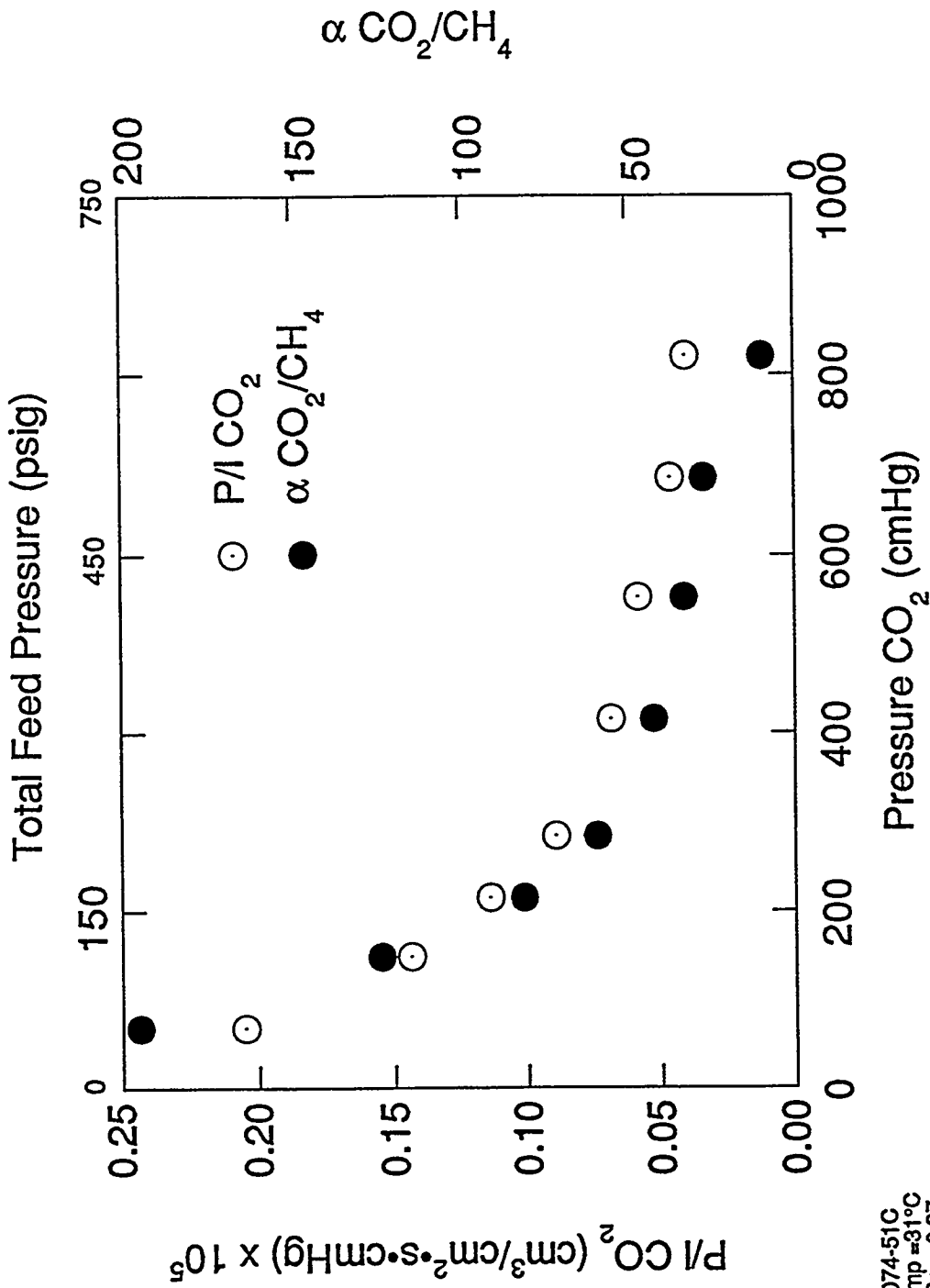
The effect of support fiber strength is shown in Figure 4-9. In this experiment, a PDMS/PVBTAf ATM was supported on SUB2 fiber. The feed pressure was incrementally raised to about 800 psig. Permselectivity parallels that of a SUB1-based ATM at low feed pressures. However, at ≈ 600 psig, the support fiber begins to collapse and membrane integrity is compromised. The composite failed completely at feed pressures greater than 650 psig. As the wall thickness of SUB2 is only about 50% that of SUB1, it is not surprising that this failure occurred. This result indicates the need to maintain the proper support fiber wall thickness to fiber OD ratio for high pressure operation.

- Effect of Bore-side Sweep Gas on Performance [13074-67C]

In order to maintain the largest driving force, the preferred mode of operating an Active Transport membrane is to sweep the fiber lumen with a diluent. However, it may not always be either technically or economically feasible to provide this option. Therefore, the performance of the hollow fiber composite module was evaluated without a permeate sweep gas. In this test, the permeate gases were collected at 15 psia and, downstream of the membrane, diluted with helium and analyzed. As expected (Figure 4-10), the lack of sweep gas only affects permselectivity at low CO₂ partial pressures. The CO₂ permeance of the non-facilitated (Henry's Law) pathway depends only on the absolute value of the CO₂ pressure difference and is not affected in the high pressure regime, where the Henry's Law pathway dominates. On the other hand, the chemical (facilitated) transport pathway dominates at low CO₂ feed pressures. The CO₂ permeance in this regime depends on the absolute values of the CO₂ partial pressure in the feed and permeate streams. Therefore, this regime shows a deviation in performance.

- P/P_o CO₂ and α CO₂/CH₄ as a function of P/P_o [13921-54]

The ATM materials development program identified a strong dependence of performance on the water content of the gas streams. This dependence was evaluated for PDMS/PVBTAf/SUB1 hollow fiber lab modules by varying the water content, as defined by P/P_o , of both the feed and sweep gas streams. The partial pressure of CO₂ in the feed stream was maintained at 53 cmHg. All other experimental parameters were held constant. Data was recorded at increasing P/P_o from 0.27 to 0.72, then performance at the lower values of P/P_o was investigated. Finally, the membrane was returned to the original conditions and

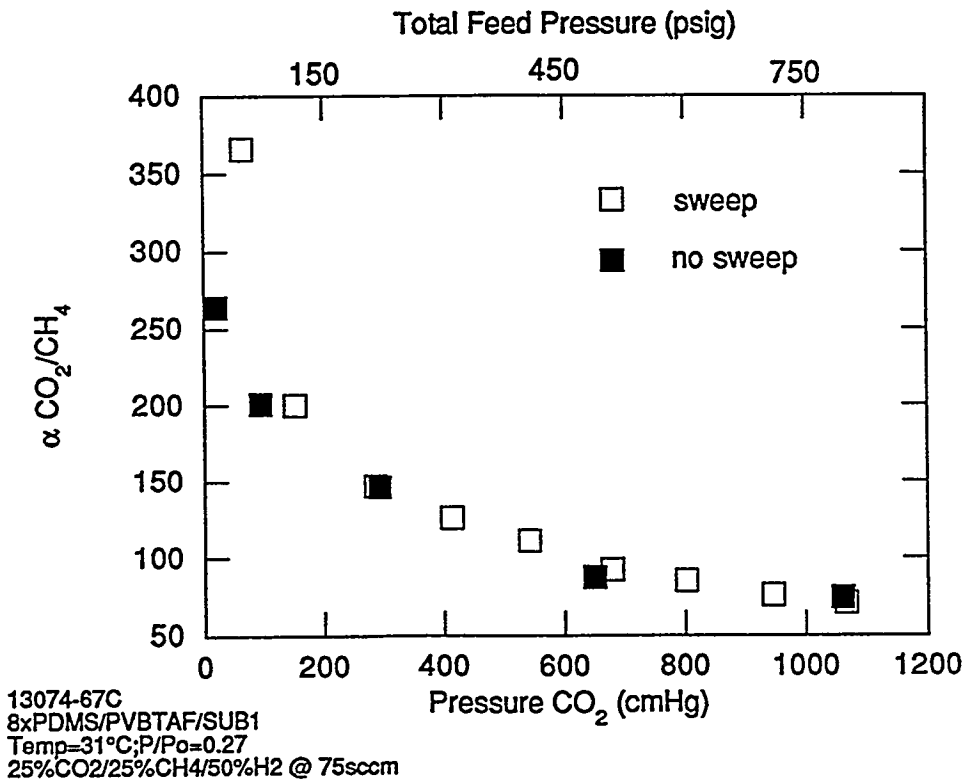
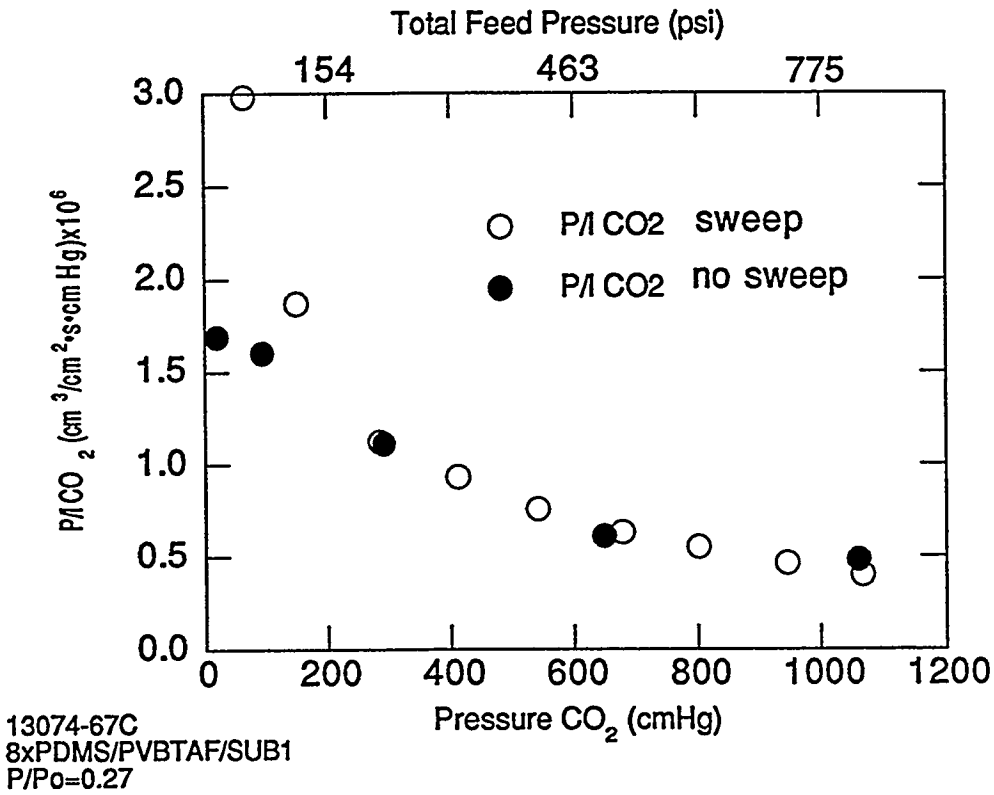


13074-51C
 Temp = 31°C
 P/Po = 0.27
 25%CO₂/25%CH₄/50%H₂ @ 75sccm

DOE4/F4-9

Figure 4-9
 Performance on SUB2 Substrate

Figure 4-10
Performance Comparison: Bore-Side Sweep vs. No Sweep



the data (represented by the filled symbols) was recorded. Results are shown in Figure 4-11. The CO₂ permeance increases linearly with increasing P/Po in the range 0.1 < P/Po < 0.75. The selectivity however, passes through a maximum. Figure 4-11 defines three regimes of membrane performance. At P/Po ≤ 0.1 both the CO₂ permeance and the selectivity are low because strong ionic intermolecular forces maintain a "tight" polymer network which inhibits diffusion of all gases. Additionally, a low water content in essence "shuts down" the chemical transport pathway in which H₂O is a reactant. An optimal regime exists in the P/Po range of 0.15 - 0.35. The CO₂/CH₄ selectivity is maximized with a moderate CO₂ permeance. At higher P/Po, excess water retards the chemical pathway and plasticizes the membrane. Thus, the flux of all gases is high and the membrane is nonselective. This aspect of ATMs is discussed in greater detail in Chapter V.

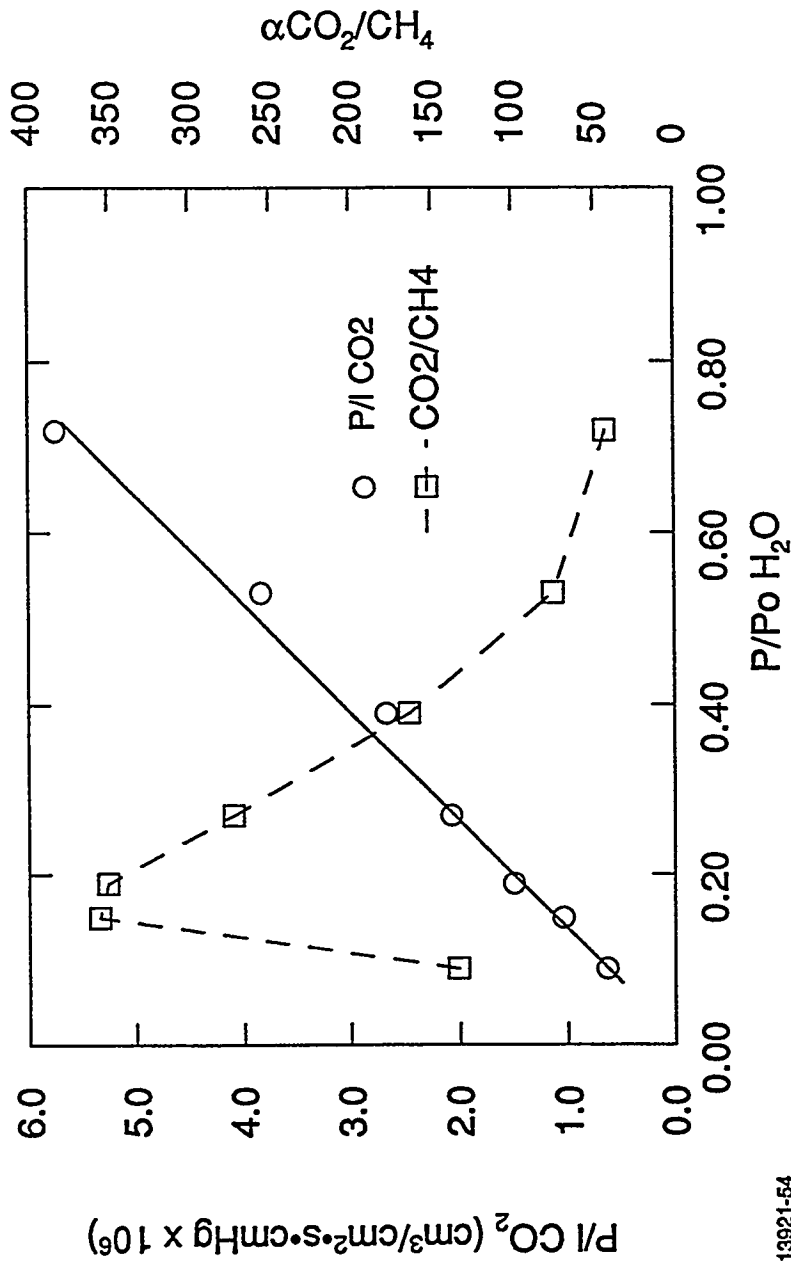
- Effect of Higher Membrane Temperature on Performance at Constant P/Po

It was found that membrane temperature can have significant effect on performance. A PDMS/PVBTAf/SUB1 module was evaluated at two temperatures, 31°C and 50°C while all other experimental parameters, including P/Po were constant. A modest 20°C temperature rise increased the observed CO₂ permeance ≈185%. Moreover, the selectivity also increased. For comparison, conventional polymeric membranes (non ATMs) usually exhibit increased permeance but decreased selectivity at higher temperatures. The results (Table 4-7) suggest better economics might be achieved if the membrane could be operated at ≈50°C. Additional experimental work is needed to define the upper temperature limit.

Table 4-7: Temperature Dependence of Permselectivity

<u>Membrane</u>	<u>P/Po</u>	<u>P/l CO₂(cm³/cm²•s•cmHg x10⁶)</u>	<u>αCO₂/CH₄</u>
31°C	0.23	3.41	185
50°C	0.23	6.27	254

conditions: 18 cmHg CO₂



DOE4/F4-11

Figure 4-11
Effect of P/Po on Performance

- Lifetime / Stability Testing and Sensitivity to H₂S-containing Gas Streams

Two types of lifetime/stability testing were investigated. In the first, a module was evaluated over a set of conditions, usually increasing feed pressure, and then re-evaluated under conditions similar to those used early in the experiment. The results of such a study are shown in Figure 4-12. After evaluation at 800 psi, the module was retested at low pressure. The results from the retest are shown in solid symbols. The original results are reproduced and, hence, the module is stable to at least limited pressure cycling. In addition, this evaluation spanned 14 days of continuous operation.

The second type of evaluation comprised a lifetime study at constant conditions for a specified period of time in order to evaluate flux creep or degradation. Additionally, various levels of H₂S, a common co-contaminant in natural gas, was also added to the feed gas to evaluate its effect on performance. Results are shown in Figure 4-13. For the first 14 days, the feed gas contained only CO₂ and CH₄. After an induction period, a steady state is reached. For days 14 - 27, a feed gas containing 2900 ppm H₂S was used. The CO₂ permeance began to decline but appeared to stabilize at about 75% of the original value. For days 28 - 36, a feed gas containing 3% H₂S was used. Again, the CO₂ permeance decreased significantly and appeared to stabilize at about 45% of the original value. There are at least two reasons for this effect. First, like CO₂, H₂S is an acid gas and competes with CO₂ for the same acid-gas reactive sites in the ATM. This competition reduces the CO₂ flux and, as a result, the CO₂/CH₄ selectivity is also reduced. The H₂S/CO₂ selectivity at this point was 10. Second, H₂S, or trace contaminants in the H₂S may react with the membrane. This reaction may involve irreversible binding to the active sites or crosslinking of the polymer network. The data from days 38 - 45 suggest both mechanisms may be operative since a return to an H₂S-free stream did not restore the CO₂ flux but did restore some of the CO₂/CH₄ selectivity. The conclusion from this study is that H₂S (or H₂S contaminant) has some detrimental and irreversible or long-lived effect on permselectivity but that a meta-stable state is achieved, the permeance of which is dependent upon the H₂S concentration.

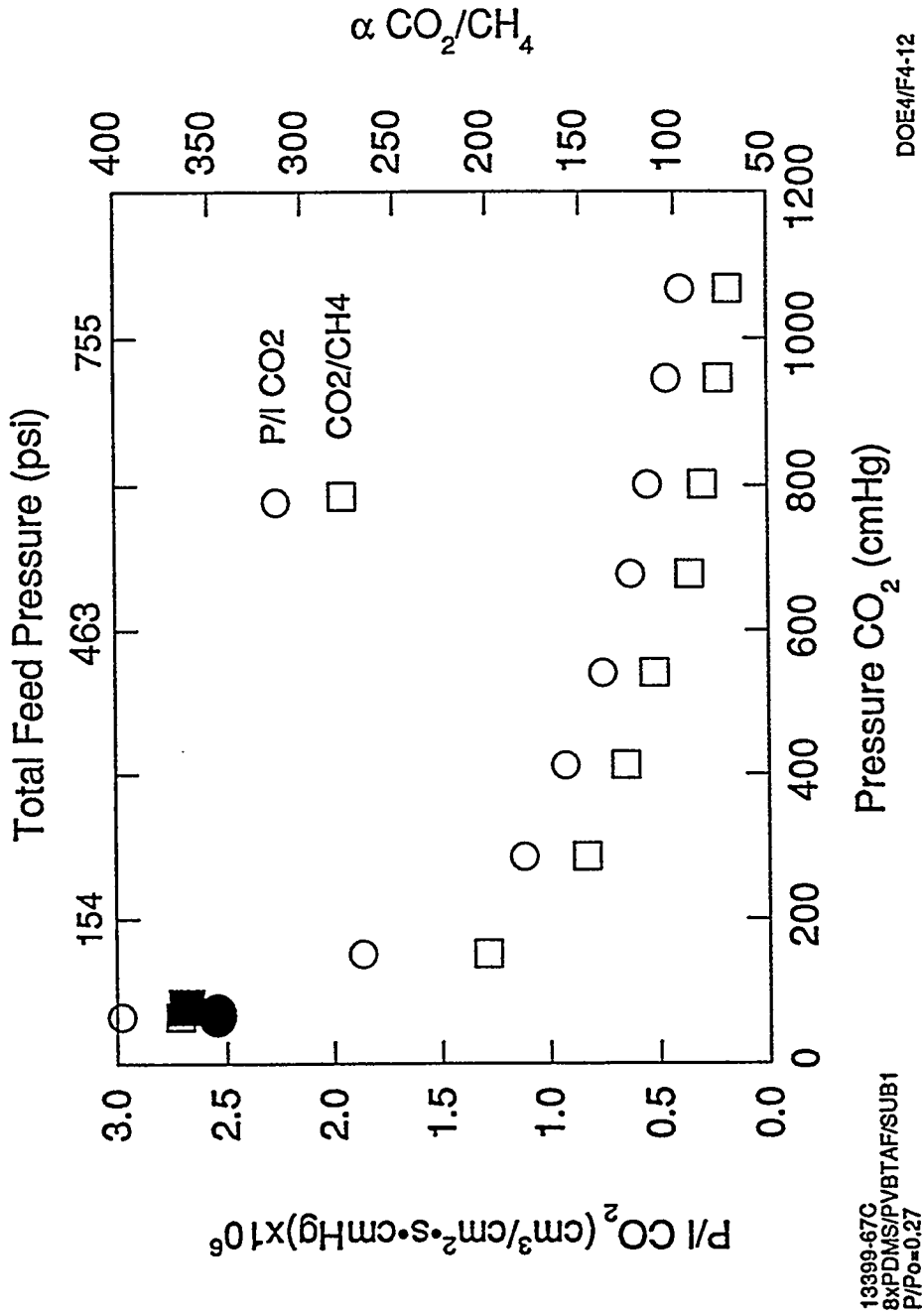


Figure 4-12:
 Stability of Lab-Scale Hollow Fiber ATM Modules

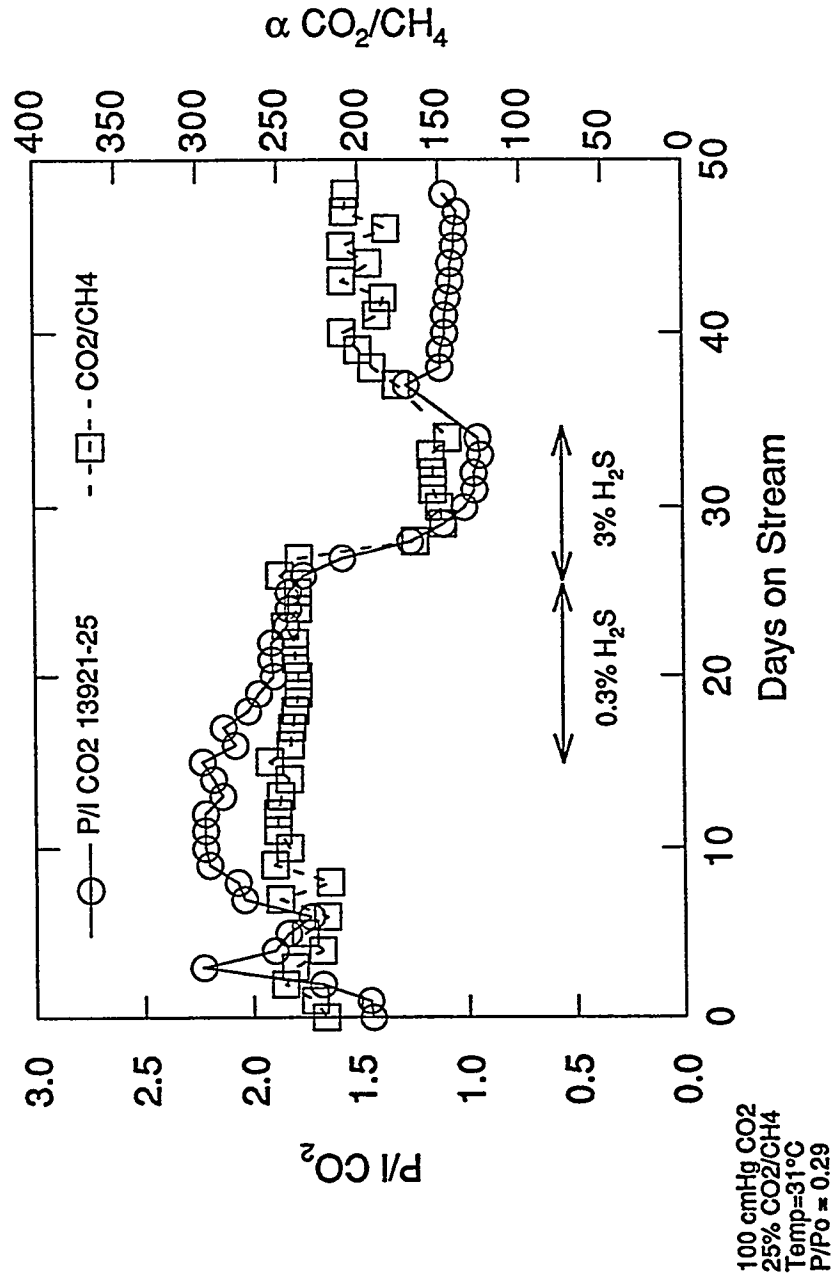


Figure 4-13
 Lifetime/H₂S Stability of Hollow Fiber ATM

- Defect Modeling of Composite ATMs

A series resistance model can be applied to explain the differences between the permselectivity of planar ATM composite membranes and hollow fiber ATM composite membranes. Table 4-8 summarizes typical laboratory properties under comparable test conditions for PVBTAF composite ATMs.

*Table 4-8
Comparison of Typical Planar and Hollow Fiber Membranes*

	<u>P/l CO₂ (x 10⁶)*</u>	<u>αCO₂/H₂</u>	<u>αCO₂/CH₄</u>
Planar Membrane	1-6	20-50	200-500
Hollow Fiber Membrane	1-5	2-10	100-300

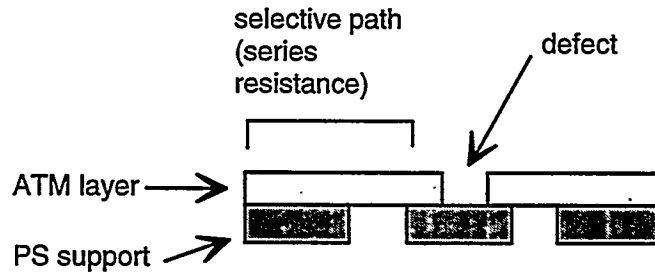
* in units of cm³/cm²•s•cmHg

Hollow fiber composite ATMs achieve CO₂ permeance and generally αCO₂/CH₄ similar to the planar counterpart however, αCO₂/H₂ is always significantly less than expected. To explain these results the following model is proposed. The model consists of the following components:

(1) A series resistance calculation to determine the intrinsic permselectivity of the PVBTAF layer from the experimentally determined properties of a planar multilayer composite membrane, the uncoated substrate (assumed to be nonporous) and the PDMS overcoat. The result is scaled to the same experimental conditions under which the hollow fiber ATM was evaluated.

(2) The defects are assumed to occur over a nonporous region of the support fiber as shown in Figure 4-14. The model then uses a two parameter fit to simultaneously solve for the ratio of the PVBTAF layer thicknesses between the planar coupon and the hollow fiber composite and the defective area. The total gas flux of any species (i) is then the sum of the flux through the coated composite of area, x, and the flux through the defect area, (1-x). These parameters are then used to predict the CH₄ permeance and αCO₂/CH₄.

Figure 4-14: Schematic Representation of Defect Model



$$(P/l)_i [\text{composite}] = L \cdot x (P/l)_i [\text{series resistance}] + (1-x) \cdot (P/l)_i \text{ defect}$$

where L = PVBTAF thickness of fiber / PVBTAF thickness of coupon
 x = defect-free area

The component permselectivities used in the calculations are given in Table 4-9.

Table 4-9
Permselectivity Basis for Defect Model

<u>Component</u>	<u>Thickness</u>	<u>P/l CO₂ (x 10⁶)*</u>	<u>P/l H₂</u>	<u>P/l CH₄</u>
substrate	1000Å	57	108	2.2
PDMS	5 μm	194	42	14

* in units of cm³/cm²•s•cmHg

An important result of the model is that neither the polysulfone (sheet or fiber) nor the PDMS overcoat provide significant mass transfer resistance to these membranes. Table 4-10 compares the experimental properties of the flat sheet ATM composite, the experimental permselectivity of a hollow fiber ATM composite and predicted (model) permselectivity for PVBTAF-coated onto SUB2 hollow fibers. The defective area was calculated at 0.17%.

Table 4-10: Comparison of Experimental and Model Predicted Permselectivity for an ATM Hollow Fiber Module ($x = 0.9983$)

<u>Property</u>	<u>PVBTAf Intrinsic Properties</u>	<u>experimental flat sheet (12484-76B)**</u>	<u>experimental hollow fiber (13074-49D)***</u>	<u>predicted (defect model)****</u>
P/l CO ₂ (x 10 ⁶)*	2.95	2.88	3.05	3.05
α CO ₂ /H ₂	44	43	12.1	12.1
α CO ₂ /CH ₄	500	490	275	316

* in units of cm³/cm²•s•cmHg

** conditions: 143 cmHg CO₂, P/Po=0.31

***conditions: 135 cmHg CO₂, P/Po=0.27

****scaled to experimental conditions of 13074-49D

Although the model is limited and does not take into account the variation in effective permeation area as the PVBTAf layer is thinned, the agreement between model and experiment is good. It provides a semi-quantitative rationalization of the experimental results and can be used to guide future work.

3.3 Results and Discussion - ATM coated PAI Substrate

This work incorporated PAI substrate developed under task 1 (Section III of this report) and new high performance ATM compositions (e.g. EXTM6-4; see Section V of this report). Planar coupons of these ATM compositions exhibited a ten-fold increase in CO₂ permeance without loss of selectivity. The performance of hollow fiber composite lab modules is reported below.

- EXTM6-4-coated PAI Substrate

Screening results for EXTM6-4 coated PAI are summarized in Table 4-11. Early results were discouraging. Eventually a procedure was developed to make largely defect free EXTM6-4 and EXTM8 coatings on small pore PAI substrate. While α (CO₂/CH₄) is good, ranging from 100-400, CO₂ permeance values are approximately that observed for PVBTAf-coated SUB1 which suggests that optimization of the PAI substrate is needed to realize the potential of the high performance ATMs. For instance, a higher CO₂ permeance was achieved on

100A pore/1500 GPU PAI (13745-5Å) compared to the <40Å pore/150 GPU PAI (13745-15B). These results demonstrate that it is possible to coat PAI with the ATM. Additional work is necessary to evaluate permselectivity under more rigorous conditions.

Table 4-11
Performance of EXTM6-4 Coated PAI Hollow Fiber Modules

<u>Reference</u>	<u>Fiber Ref</u>	<u>P/Po</u>	<u>P CO₂</u> *	<u>P/CO₂</u> **	<u>α CO₂/CH₄</u>
13921-83	90B	0.38	98	1.1	240
		0.52	106	1.4	153
		0.27	103	0.79	159
13921-85	13475-15B	0.28	50	1.4	227
		0.30	50	0.94	399
		0.40	124	0.65	133
		0.36	124	0.66	178
13921-94	13475-5A	0.29	125	2.1	274
		0.4	125	2.6	237

* cmHg

** units of $10^{-6} \text{ cm}^3/\text{cm}^2 \cdot \text{s} \cdot \text{cmHg}$

• EXTM8-Coated PAI Substrate

Table 4-12 summarizes results for EXTM8-coated PAI. Here too, EXTM8 based composites exhibit high selectivity but not the expected improved CO₂ permeance. These results re-emphasize the need to optimize the support fiber. It is worth noting that in some cases Rayleigh instability³⁷ was observed during the coating process and may be an issue in EXTM8 coating scale-up.

³⁷D. Quere et. al., "Spreading of Liquids on Highly Curved Surfaces", *Science*, 249, 1256-1259 (1990).

EXTM8-Coated PAI Fibers
 Feed gas: 25% CO₂, 25% CH₄, 50% H₂ @ 75sccm

Fiber #	Ref.#	P/Po	P.CO ₂	P/CO ₂	CO ₂ /CH ₄	t _{on-stream}	Comment
69A	13074-93B	0.27	83	4.7	321	96 hrs	
		0.27	153	3.3	1325		
		0.27	272	2.2	637		
69A	13074-94E	0.27	88	3.4	485	64 hrs	
		0.21	88	2.0	22		
		0.27	98	3.3	50		
		0.38	98	3.8	292		
69A	13074-100	0.27	162	6.5	1.1	3 hrs	
69A	13074-101	0.27	162	2.4	22.3	5 hrs	
		0.27	162	21.9	0.8		
69A	13074-102	0.27	162	23.2	0.9	24 hrs	
		0.27	162	29.9	0.9		
69A	13074-103	0.38	92	4.0	1.1	4 hrs	recoated in housing
		0.38	124	0.41	7.5	4 hrs	
69A	13399-1	0.27	124	3.2	8.6	4 hrs	recoated in housing
		0.38	149	1.9	3.8		
		0.52	149	1.4	13.8	20 hrs	
38A	13399-2	0.27	124	60.3	1.0	4 hrs	
38A	13399-3	0.27	124	14.4	1.1	4 hrs	
69A	13399-4	0.27	147	10.7	1.1	4 hrs	
69A	13399-5	0.27	149	11.1	1.1	4 hrs	no sweep
69A	13399-10	0.27	89	1.2	1.1	4 hrs	

Table 4-12
Summary: Permselectivity of EXTM8-coated PAI Modules

<u>Fiber #</u>	<u>Ref #</u>	<u>P/P₀</u>	<u>P/CO₂</u>	<u>P/CO₂</u>	<u>P/CO₂</u>	<u>CO₂/CH₄</u>	<u>T_{on stream}</u>	<u>Comment</u>
69A	13399-13	0.27 0.38 0.52 0.52	84 84 79 160	1.6 2.0 2.3 1.8	38.8 83.0 292 5.0	96 hrs		
69A	13399-14	0.27 0.52 0.52 0.38 0.52	91 91 156 92 96	1.7 1.9 1.8 2.1 2.0	11.2 117.2 38.4 82.1 129	148 hrs		
69A	13399-18	0.52	92	2.5	24	4 hrs		
69A	13399-19	0.52 0.52 0.52 0.38 0.52	87 88 157 157 157	3.5 3.5 2.9 2.8 3.0	199 270 53 21.2 48.9	72 hrs		
69A	13399-22	0.52	88	3.6	2.3	4 hrs		
69A	13399-23	0.52	88	3.0	9.1	4 hrs		
69A	13399-25	0.52	92	3.1	10.7	4 hrs		
69A	13399-26	0.52	91	2.9	140	14 hrs		
69A	13399-27	0.52 0.52 0.38 0.38 0.27 0.38 0.38 0.38	91 88 89 170 170 170 296 245	1.5 1.7 0.85 0.61 0.21 0.45 0.31 202	133 117 454 249 ??? 308 273 1.1	270 hrs	failure at 185 psig	

Table 4-12 (cont'd)

<u>Fiber#</u>	<u>Ref.#</u>	<u>P/Po</u>	<u>P.CO2</u>	<u>P/CO2</u>	<u>CO2/CH4</u>	<u>T.on_stream</u>	<u>Comment</u>
69B	13399-28	0.38 0.52 0.71 0.52	88 91 91 84	3.8 2.8 2.4 2.3	16.7 26.9 84.1 32.8	148 hrs	
68C	13399-45	0.34	95	4.1	2.4	4 hrs	wiped fiber
12932-68C	13399-48	0.34	92	20.0	1.5	4 hrs	
12932-68C	13399-50	0.38	95	5.6	1.8	4 hrs	

Table 4-12 (cont'd)

4.0 Summary and Recommendations

Figure 4-15 summarizes typical results for polysulfone-supported PVBTAF planar coupons and hollow fiber lab modules. The CO₂ permeance of the coupons and modules agree to within 25-40%. The selectivity of the modules is less than that observed on coupons, probably for the reasons stated above, but is acceptable and significantly higher than that of any conventional polymer membrane.

Thus far, dip coating procedures have been used to fabricate laboratory scale modules. The ATM layer thickness of the lab modules is 2-10 μm. It will be necessary to translate these results into a continuous coating process as part of a scale-up program. In addition, methods to increase the CO₂ permeance of the module, through fundamental improvements to ATM chemistry, advanced coating technology and innovative module design should be explored, particularly the effect of substrate porosity on performance. A follow-on program should include:

- determine module performance and stability at $P/P_o < 0.2$ and $P/P_o > 0.7$.
- examine methods to produce thinner coatings and determine the effect of coating thickness on flux
- scale-up a continuous coating process
- field test ATM substrates and composite membrane modules